Electronic Supplementary Material (ESI) for Chemical Communications

Supporting information

Development of a Tailor-made Bis(oxazolidine)pyridine-metal catalyst for the [3+2] Cycloaddition of Azomethine Imines with Propiolates

Takayoshi Arai*, Yuta Ogino, Toru Sato

Department of Chemistry, Graduate School of Science, Chiba University

Inage, Chiba 263-8522, Japan.

Contents

1. General

Infrared (IR) spectra were recorded on a JASCO FT/IR-4100 Fourier transform infrared spectrophotometer. NMR spectra were recorded on a JEOL JNM-ECA500 or JEOL JNM-ECA400 spectrometer, operating at 500 MHz or 400 MHz for ^{1}H-NMR and 125 MHz or 100 MHz for ^{13}C-NMR. Chemical shifts in $CDCl_3$ were reported downfield from TMS (=0 ppm) for ^{1}H-NMR. For ^{13}C-NMR, chemical shifts were reported downfield from TMS (=0 ppm) or in the scale relative to $CHCl_3$ (77.00 ppm for ^{13}C-NMR) as an internal reference. Optical rotations were measured on a JASCO P-1020 Polarimeter. The enantiomeric excess (*ee*) was determined by HPLC analysis. Column, DAICEL CHIRALPAK AD-H, OD-H; mobile phase, hexane-*i*-PrOH; flow rate, 1.0 mL/min. General experimental details for synthesis of PyBidine ligand see reference 4 in the manuscript. Azomethine imines were synthesized according to the literature procedure [2].

1) T. Arai, A. Mishiro, N. Yokoyama, K. Suzuki and H. Sato, *J. Am. Chem. Soc.,* 2010, **132**, 5338.

2) R. Shintani and G. C. Fu, *J. Am. Chem. Soc.,* 2003, **125**, 10778.

2. Synthesis of 4-(3-hydroxypropoxy)pyridine-2,6-dicarbaldehyde

The 4-(3-hydroxypropoxy)pyridine-2,6-dicarbaldehyde (**E**) was synthesized by following Scheme.

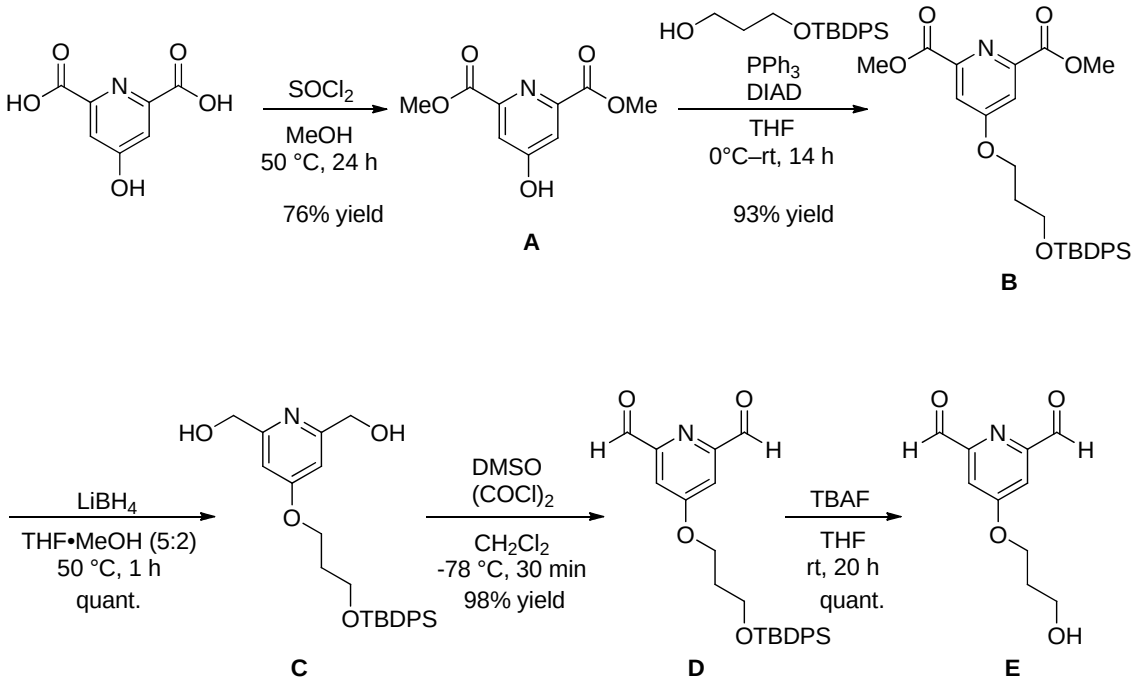

Synthesis of dimethyl 4-hydroxypyridine-2,6-dicarboxylate (**A**)

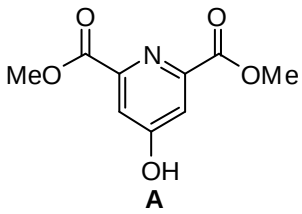

Chelidamic acid monohydrate (12.3 mmol) was added to a round flask containing a stir bar. After dissolving in MeOH (30 ml), thionyl chloride (24.6 mmol) was added, and stirred 24 hours at 50 °C. The mixture was quenched by adding potassium carbonate aqueous, and extracted with CH_2Cl_2. The resulting solution was concentrated in *vacuo* to afford a product **A**.

Dimethyl 4-hydroxypyridine-2,6-dicarboxylate (**A**)

^{1}H NMR (400 MHz, DMSO-d_6) δ 11.59 (s, 1H), 7.56 (s, 2H), 3.86 (s, 6H); ^{13}C NMR (400 MHz, DMSO-*d6*) δ 166.3, 165.2, 149.7, 115.7, 53.0; HRMS (ESI) calcd for $C_9H_{10}NO_5$ $[M + H]^+$ 212.0554; found, 212.0552. These data were identical to those previously reported.[3)]

3) Zeng, T.; Yang, L.; Hudson, R.; Song, G.; Moores A. R.; Li, C.-J. *Org. Lett*. **2011**, *13*, 442–445.

Synthesis of dimethyl 4-(3-((*tert*-butyldiphenylsilyl)oxy)propoxy)pyridine-2,6-dicarboxylate (**B**)

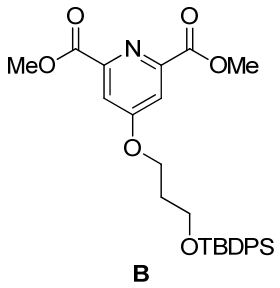

B

A mixture of **A** (4.95 mmol), 3-((*tert*-butyldiphenylsilyl)oxy)propan-1-ol (5.94 mmol), and PPh_3 (5.94 mmol) was dissolved to THF (25 ml) in a round flask containing a stir bar. To the solution, DIAD (5.94 mmol) was added dropwise at 0 °C and was stirred 14 hours at rt. The resulting solution was concentrated in *vacuo*, and purified by column chromatography (hexane:AcOEt = 3:1) to afford product **B**.

Dimethyl 4-(3-((*tert*-butyldiphenylsilyl)oxy)propoxy)pyridine-2,6-dicarboxylate (**B**)

FTIR (neat) 3324, 2930, 2883, 2855, 1717, 1597, 1452, 1369, 1345, 1251, 1100, 1070, 1033, 1005, 883, 822, 785, 736, 700 cm^{-1}; ^1H NMR (400 MHz, $CDCl_3$) δ 7.76 (s, 2H), 7.64-7.61 (m, 4H), 7.62-7.28 (m, 6H), 4.26 (t, *J*= 6.0 Hz, 2H), 4.02 (s, 6H), 3.86 (t, *J*= 6.0 Hz, 2H), 2.07-2.03 (pentet, *J*= 6.0 Hz, 2H), 1.04 (s, 9H); ^{13}C NMR (100 MHz, $CDCl_3$) δ 166.9, 165.1, 149.6, 135.4, 133.4, 129.6, 127.6, 114.4, 65.4, 59.5, 53.1, 31.5, 26.8, 19.1; HRMS (ESI) calcd for $C_{28}H_{34}NO_6Si$ $[M + H]^+$ 508.2150; found, 508.2137.

Synthesis of (4-(3-((*tert*-butyldiphenylsilyl)oxy)propoxy)pyridine-2,6-diyl)dimethanol (**C**)

To the solution of **B** (4.31 mmol) in THF-MeOH (5:2) (22 ml) was $LiBH_4$ slowly at 0 °C. The mixture was stirred 1 h at 50 °C. The resulting mixture was diluted by water and extracted with $CHCl_3$. After evaporation, the residue was purified by column chromatography (hexane:AcOEt = 3:1 to 0:1) to afford product **C**.

(4-(3-((*tert*-butyldiphenylsilyl)oxy)propoxy)pyridine-2,6-diyl)dimethanol (**C**)

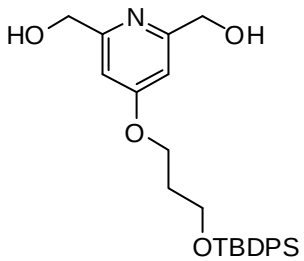

C

FTIR (neat) 3364, 3065, 2926, 1606, 1455, 1301, 1158, 1077, 741, 701 cm^{-1}; ^1H NMR (400 MHz, $CDCl_3$) δ 7.64-7.62 (m, 4H), 7.43-7.26 (m, 6H), 6.67 (s, 2H), 4.70 (s, 4H), 4.18 (t, *J*= 6.0 Hz, 2H), 3.84 (t, *J*= 6.0 Hz, 2H), 2.02 (pentet, *J*= 6.0 Hz, 2H), 1.03 (s, 9H); ^{13}C NMR (100 MHz, $CDCl_3$) δ 166.5, 160.1, 135.5, 133.6, 129.7, 127.7, 105.5, 64.7, 64.4, 59.9, 31.8, 26.8, 19.2; FTMS (ESI) calcd for $C_{26}H_{34}NO_4Si$ $[M + H]^+$ 452.2019; found, 452.2250.

Synthesis of 4-(3-((*tert*-butyldiphenylsilyl)oxy)propoxy)pyridine-2,6-dicarbaldehyde (**D**)

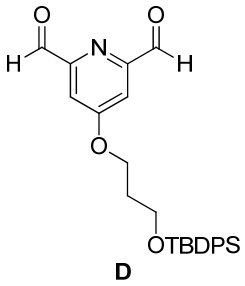

D

Oxalyl chloride (6.51 mmol) and CH_2Cl_2 were added to a round flask under Ar. The solution was stirred several minutes at -78 °C. DMSO (14.09 mmol) in CH_2Cl_2 was added slowly to the flask, and **C** (2.71 mmol) (CH_2Cl_2 solution) was added to the flask. After stirring 30 min at -78 °C, Et_3N (27.10 mmol) was added to the flask, and stirred for 30 min at rt. The resulting mixture was diluted by water and extracted with CH_2Cl_2. The concentrated residue was dried *in vacuo* to afford product **D**.

4-(3-((*tert*-butyldiphenylsilyl)oxy)propoxy)pyridine-2,6-dicarbaldehyde (**D**)

FTIR (neat) 3413, 3071, 2957, 2857, 1714, 1594, 1449, 1365, 1313, 1111, 702 cm^{-1}; ^1H NMR (400 MHz, $CDCl_3$) δ 10.12 (s, 2H), 7.64-7.60 (m, 4H), 7.57 (s, 2H), 7.42-7.32 (m, 6H), 4.26 (t, *J*= 6.0 Hz, 2H), 3.86 (t, *J*= 6.0 Hz, 2H), 2.06 (pentet, *J*= 6.0 Hz, 2H), 1.03 (s, 9H); ^{13}C NMR (125 MHz, $CDCl_3$) δ 192.4, 167.0, 154.7, 135.5, 133.4, 129.7, 127.7, 111.4, 65.7, 59.6, 46.2, 31.6, 26.8, 19.2; HRMS (ESI) calcd for $C_{26}H_{30}NO_4Si$ $[M + H]^+$ 448.1939; found, 448.1939.

Synthesis of 4-(3-hydroxypropoxy)pyridine-2,6-dicarbaldehyde (**E**)

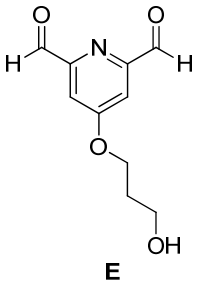

E

To the compound **D** (2 mmol) in a round flask was added tetra butyl ammonium fluoride (1 mol/L THF solution) (3 ml) and the resulting mixture was stirred 20 hours at rt. The resulting solution was diluted with water and extracted with $CHCl_3$. The residue was dried in vacuo to afford a product (**E**) as a mixture with tetra butyl ammonium.

4-(3-hydroxypropoxy)pyridine-2,6-dicarbaldehyde (**E**)

^1H NMR (400 MHz, $CDCl_3$) δ 10.11 (s, 2H), 7.66 (s, 2H), 4.32 (t, *J*= 6.1 Hz, 2H), 3.88 (t, *J*= 6.1 Hz, 2H), 2.11 (pentet, *J*= 6.1 Hz, 2H); ^{13}C NMR (100 MHz, $CDCl_3$) δ 192.5, 167.1, 154.8, 111.6, 66.2, 59.1, 31.5.

3. Synthesis of polymer-supported PyBodines-Cu catalysts and Solid-phase catalysis/CD-HTS

*Immobilization of compound **E** on the polystyrene beads*:

To the (4-Methoxyphenyl)diisopropylsilylpropyl polystyrene beads (loading: 1.4 mmol/g, purchased from NovaBioChem) (286 mg, 0.4 mmol) in a 10 mL polystyrene column, 7.6 ml of a 3% TfOH/CH_2Cl_2 solution (5 equiv. of TfOH) was added by syringe. The resin turned bright red upon acid treatment and was the gently agitated for 30 min under Ar atmosphere to get the Si-OTf functionality. Once activation was completed, excess acid was removed by washing with CH_2Cl_2 under Ar atmosphere. Then, a treatment of the beads with 2,6-lutidine (0.37 mL, 8 equiv. relative to Si-OTf) followed by addition of **E** (176 mg, 0.8 mmol) resulted yellow resin. After the gentle agitation of the reaction mixture for 15 h under Ar atmosphere, the filtrated beads were washed with CH_2Cl_2. The resulting beads were dried *in vacuo.*

Preparation of polymer-supported PyBodines-Cu catalysts and asymmetric [3+2]-cycloaddition:

The polystyrene beads (8.0 mg) were swollen in CH_2Cl_2 (0.5 ml) for 30 min at room temperature in a solvent-resistant scintillation vial. To the swollen beads, amino alcohol (10 equiv. relative to the compound **E** on the polystyrene beads) was added. After the gentle agitation of the reaction mixture for 15 h under Ar atmosphere, the filtrated beads were washed with CH_2Cl_2. The resulting beads dried *in vacuo* were used as the polymer-supported PyBodines. To the polymer-supported PyBodines, copper salt (0.05 mmol, ca. 1.0 eq. to PyBodines) [CuOAc (0.6 mg), $Cu(OAc)_2$ (0.9 mg), CuI (1.0 mg)] was added in CH_2Cl_2 (0.5 mL) for 30 h. The resulting beads were washed with CH_2Cl_2, and dried *in vacuo*. To the polymer supported PyBodines-Cu catalysts in CH_2Cl_2 (0.5 mL), **1a** (8.71 mg, 0.05 mmol) and **2a** (6.0μl, 0.06 mmol) were added. After carrying out the asymmetric reaction at rt for 11 h, the reaction mixtures were analyzed by the solid-phase catalysis/CD-HTS.

Solid-phase catalysis/CD-HTS:

HTS system was constructed with an autosampler (JASCO AS-2057), a pump (JASCO PU-2080), and a CD-detector (JASCO CD-2095). A line between the auto sampler and the CD-detector was connected by Teflon tube as shown in the picture. For the CD-HTS examined in Figure 3 of the manuscript, the sample was prepared by a dilution of 25 μl of the reaction mixture with 950 μl of an eluent (*i*PrOH/Hex = 1/9). In each period of 3 min interval, 5 μl of the sample was injected, and the CD was operated at 254nm (flow rate: 0.5 mL/min). The CD data was analyzed by using JASCO-BOWIN program.

4. General procedure for the preparation of PyBodines and the analytical dada

Synthesis of PyBodines:

To a solution of 2,6-pyridine dicarboxyaldehyde (0.5 mmol) in CH_2Cl_2 (2 mL) was added amino alcohol (1 mmol), and the mixture was stirred at rt for 6 hours. The resulting solution was concentrated *in vacuo* to afford adduct.

[Analytical dada of PyBodines]

2,6-bis((2R,4S)-4-methyl-5,5-diphenyloxazolidin-2-yl)pyridine

FTIR (neat) 2952, 2922, 2853, 1458, 939, 700 cm^{-1}; ^1H NMR (400 MHz, DMSO-d_6) δ 8.09 (t, J = 7.7 Hz, 1H), 7.82 (d, J = 7.7 Hz, 2H), 7.51-7.50 (m, 4H), 7.44-7.40 (m, 4H), 7.35-7.31 (m, 6H) 7.17-7.10 (m, 6H), 5.62 (d, J = 12.6 Hz, 2H), 4.20-4.16 (m, 2H), 3.69 (t, J = 12.6 Hz, 2H), 1.04 (d, J = 6.6 Hz, 6H); ^{13}C NMR(125 MHz, $CDCl_3$) δ 155.3, 145.7, 143.6, 138.2, 128.2, 127.5, 127.3, 127.1, 126.7, 124.5, 90.6, 88.2, 63.7, 53.4, 18.1; FTMS (ESI) calcd for $C_{37}H_{36}N_3O_2$ $[M + H]^+$ 554.2808; found, 554.2806; $[\alpha]_D^{26}$ −82.1 (*c* 1.01, $CHCl_3$).

2,6-bis((4S)-4-isopropyl-5,5-diphenyloxazolidin-2-yl)pyridine

FTIR 2956, 2924, 2854, 1456, 1377, 1003, 938, 813, 755, 728, 700 cm^{-1}; ^1H NMR (400 MHz, DMSO-*d6*) δ 8.06 (t, J = 7.6Hz, 1H), 7.76 (d, J = 7.6Hz, 2H), 7.44-7.36 (m, 8H), 7.31-7.28 (m, 2H) 7.23-7.19 (m, 4H), 7.13-7.11 (m, 6H), 5.54 (d, J = 12.5 Hz, 2H), 3.89 (dd, J = 12.5, 3.4 Hz, 2H), 3.75 (t, J = 12.5 Hz, 2H), 1.92-1.85 (m, 2H), 1.08 (d, J = 6.7 Hz, 6H), 0.15 (d, J = 6.7 Hz, 6H) ; ^{13}C NMR (125 MHz, $CDCl_3$) δ 155.0, 146.4, 143.8, 138.1, 128.1, 127.8, 127.6, 127.5, 127.2, 126.7, 124.6, 90.2, 88.0, 73.0, 28.6, 23.3, 16.8; FTMS (ESI) calcd for $C_{41}H_{44}N_3O_2$ $[M + H]^+$ 610.3434; found, 610.3434; $[\alpha]_D^{26}$ −42.9 (*c* 1.05, $CHCl_3$).

2,6-bis((3R,7aS)-1,1-diphenylhexahydropyrrolo[1,2-c]oxazol-3-yl)pyridine

FTIR (neat) 2925, 2854, 1462, 1446, 1377, 1006, 701 cm^{-1}; ^{1}H NMR (400 MHz, $CDCl_3$) δ 7.94-7.88 (m, 3H), 7.59 (d, *J* = 7.2 Hz, 4H), 7.49 (d, *J* = 7.2 Hz, 4H), 7.35-7.17 (m, 12H), 5.59 (s, 2H), 4.59 (brs, 2H), 2.58-2.47 (m, 4H), 1.87-1.80 (m, 2H), 1.64-1.48 (m, 4H), 1.34-1.26 (m, 2H); ^{13}C NMR(100 MHz, $CDCl_3$) δ 156.44, 145.50, 144.01, 136.68, 128.19, 127.97, 127.23, 126.45, 126.17, 121.07, 91.75, 88.11, 72.48, 48.84, 29.92, 25.99; FTMS (ESI+) calcd for $C_{41}H_{40}N_3O_2$ $[M + H]^+$ 606.3121; found 606.3118; $[\alpha]_D^{26}$ −177.6 (*c* 1.14, $CHCl_3$).

5. General procedure of PyBodine (Ala)-$Cu(OAc)_2$ catalyzed [3+2]-cycloaddition and the analytical data of cycloadducts

General procedure of [3+2]-cycloaddition:

PyBodine (Ala) (0.015 mmol) and $Cu(OAc)_2$ (0.0165 mmol) were added to a round flask containing a stir bar under Ar. CH_2Cl_2 (1 mL) was added to the flask and the mixture was stirred over 12 hours. To the resulting solution was added azomethine imine (0.15 mmol) and 4A MS (75 mg) at rt. After cooling to –40 °C, to the mixture was added ethyl propiolate (0.18 mmol). After stirring for appropriate time, the reaction mixture was purified by silica gel column chromatography (Et_2O/Hexane=2/1 to Et_2O) to afford cycloadduct.

[Analytical data of cycloadducts]

(R)-ethyl 5-oxo-1-phenyl-1,5,6,7-tetrahydropyrazolo[1,2-a]pyrazole-2-carboxylate

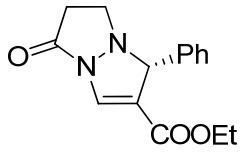

Yellow oil; FTIR (neat) 3087, 3031, 2980, 2928, 2853, 1699, 1602, 1433, 1414, 1388, 1364, 1321, 1251, 1206, 1173, 1104, 1039, 842, 752, 700 cm^{-1}; ^1H NMR (400 MHz, $CDCl_3$) δ 7.54 (d, *J* =0.5 Hz, 1H), 7.44-7.25 (m, 5H), 5.15 (d, *J* =1.7 Hz, 1H), 4.15-3.95 (m, 2H) 3.41-3.36 (m, 1H) 3.08-3.00 (m, 1H) 2.95-2.83 (m, 1H), 2.79-2.70 (m, 1H), 1.13 (t, *J* =7.2 Hz, 3H); ^{13}C NMR (100 MHz, $CDCl_3$) δ 164.7, 163.4, 138.2, 128.5, 128.4, 128.3, 128.2, 118.5, 73.3, 60.4, 51.6, 35.7, 14.0; HRMS (ESI) Calcd for $C_{15}H_{16}N_2O_3Na^+$ $[M + Na]^+$: 295.1053; Found, 295.1048; The enantiomeric excess of (*R*)-ethyl-5-oxo-1-phenyl-1,5,6,7-tetrahydropyrazolo[1,2-a]pyrazole-2-carboxylate was determined by chiral stationary-phase HPLC analysis [DAICEL CHIRALPAK AD-H, *i*-PrOH/hexane 20/80, flow rate 1.0 mL/min, t_R 10.7 min (major, 97%) and 13.1 min (minor, 3%), detection at 330 nm]; $[\alpha]_D^{23}$ −371 (*c* 0.57, $CHCl_3$).

(R)-ethyl 5-oxo-1-(p-tolyl)-1,5,6,7-tetrahydropyrazolo[1,2-a]pyrazole-2-carboxylate

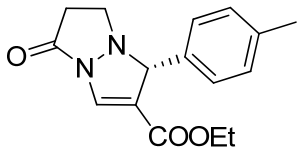

Yellow oil; FTIR (neat) 3083, 3067, 2975, 2924, 2844, 1696, 1600, 1514, 1436, 1364, 1320, 1252, 1209, 1103,1028, 813, 782 cm^{-1}; ^1H NMR (500 MHz, $CDCl_3$) δ 7.53 (s, 1H), 7.25 (d, *J*=8.6 Hz, 2H), 7.17 (d, *J* =7.7 Hz, 2H), 5.13 (s, 1H), 4.13-4.02 (m, 2H), 3.36 (m, 1H), 3.05-3.00 (m, 1H), 2.91-2.84 (m, 1H), 2.78-2.73 (m, 1H), 2.34 (s, 3H), 1.15 (t, *J*=7.2 Hz, 3H); ^{13}C NMR (125 MHz, CDCl3) δ 164.5, 163.4, 138.2, 135.1, 129.2, 128.3, 128.1, 118.5, 72.9, 60.3, 51.3, 35.7, 21.1, 14.0; HRMS (ESI) Calcd for $C_{16}H_{18}N_2O_3^+$ $[M + H]^+$: 287.1390; Found, 287.1389; The enantiomeric excess of (*R*)-ethyl 5-oxo-1-(p-tolyl)-1,5,6,7-tetrahydropyrazolo[1,2-a]pyrazole-2-carboxylate was determined by chiral stationary-phase HPLC analysis [DAICEL CHIRALPAK AD-H, *i*-PrOH/hexane 20/80, flow rate 1.0 mL/min, t_R 8.2 min (major, 95%) and 9.4 min (minor, 5%), detection at 330 nm]; $[\alpha]_D^{24}$ −312 (*c* 0.44, $CHCl_3$).

(R)-ethyl 5-oxo-1-(o-tolyl)-1,5,6,7-tetrahydropyrazolo[1,2-a]pyrazole-2-carboxylate

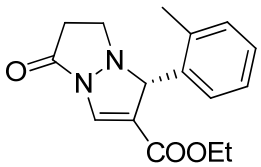

Yellow oil; FTIR (neat) 3099, 2985, 2860, 1692, 1600, 1416, 1362, 1319, 1248, 1098, 751, 665 cm^{-1}; ^1H NMR (500 MHz, $CDCl_3$) δ 7.56 (s, 1H), 7.32-7.30 (m, 1H), 7.22-7.16 (m, 3H), 5.48 (d, *J*=1.4 Hz, 1H), 4.10-4.00 (m, 2H), 3.35 (m, 1H), 3.10-3.04 (m, 1H), 2.86-2.84 (m, 1H), 2.78-2.74 (m, 1H), 2.45 (s, 3H), 1.12 (t, *J*=7.2 Hz, 3H); ^{13}C NMR (125 MHz, CDCl3) δ 164.7, 163.3, 136.5, 135.9, 130.7, 128.52, 128.46, 128.1, 126.3, 118.7, 69.3, 60.4, 51.6, 35.7, 25.3, 19.4, 14.0; HRMS [ESI] Calcd for $C_{16}H_{18}N_2O_3^+$ $[M + H]^+$: 287.1390; Found, 287.1387; The enantiomeric excess of (*R*)-ethyl 5-oxo-1-(*o*-tolyl)-1,5,6,7-tetrahydropyrazolo[1,2-a]pyrazole-2-carboxylate was determined by chiral stationary-phase HPLC analysis [DAICEL CHIRALPAK AD-H, *i*-PrOH/hexane 5/95, flow rate 1.0 mL/min, t_R 23.9 min (minor, 2.7%) and 27.7 min (major, 97.3%), detection at 330 nm]; $[\alpha]_D^{24}$ −338 (*c* 0.21, $CHCl_3$).

(R)-ethyl 1-(3-chlorophenyl)-5-oxo-1,5,6,7-tetrahydropyrazolo[1,2-a]pyrazole-2-carboxylate

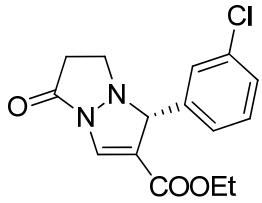

Yellow oil; FTIR (neat) 3086, 2981, 2927, 2851, 1697, 1599, 1433, 1363, 1319, 1248, 1198, 1171, 1105, 1024, 763 cm^{-1}; ^1H NMR (400 MHz, $CDCl_3$) δ 7.53 (s, 1H), 7.42 (s, 1H), 7.30 (d, *J* =1.4 Hz, 3H), 5.12 (d, *J* =1.8 Hz, 1H), 4.15-3.95 (m, 2H), 3.50-3.45 (m, 1H), 3.09-3.02 (m, 1H), 2.98-2.89 (m, 1H), 2.78-2.72 (m, 1H), 1.16 (t, *J* =7.2 Hz, 3H); ^{13}C NMR (100 MHz, $CDCl_3$) δ 164.7, 163.2, 140.9, 134.4, 129.6, 128.7, 128.5, 128.3, 126.5, 73.0, 60.5, 52.1, 35.5, 14.0; HRMS (ESI) Calcd for $C_{15}H_{16}N_2O_3Cl^+$ $[M + H]^+$: 307.0844; Found, 307.0839; The enantiomeric excess of *(R)*-ethyl 1-(3-chlorophenyl)-5-oxo-1,5,6,7-tetrahydropyrazolo[1,2-a]pyrazole-2-carboxylate was determined by chiral stationary-phase HPLC analysis [DAICEL CHIRALPAK AD-H, *i*-PrOH/hexane 20/80, flow rate 1.0 mL/min, t_R 9.1 min (major, 97%) and 11.1 min (minor, 3%), detection at 330 nm]; $[\alpha]_D^{24}$ −462 (*c* 0.23, $CHCl_3$).

(R)-ethyl 1-(4-fluorophenyl)-5-oxo-1,5,6,7-tetrahydropyrazolo[1,2-a]pyrazole-2-carboxylate

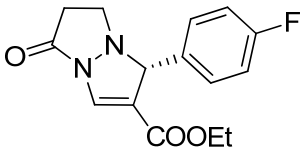

Yellow oil; FTIR (neat) 3083, 2982, 2933, 2850, 1696, 1604, 1509, 1433, 1364, 1320, 1251, 1172, 1106, 849 cm^{-1}; ^1H NMR (500 MHz, CDCl3) δ 7.53 (s, 1H), 7.40-7.36 (m, 2H), 7.07-7.04 (m, 2H), 5.14 (d, *J*=1.7 Hz, 1H), 4.13-4.02 (m, 2H), 3.43 (m, 1H), 3.07-3.02 (m, 1H), 2.95-2.88 (m, 1H), 2.79-2.73 (m, 1H), 1.15 (t, *J*=7.2 Hz, 3H); ^{13}C NMR (125 MHz, $CDCl_3$) δ 164.6, 163.3, 134.4, 129.9, 129.8, 128.5, 118.2, 115.5, 115.3, 60.5, 51.8, 35.7, 14.0; HRMS (ESI) Calcd for $C_{15}H_{15}N_2FO_3^+$ $[M + H]^+$: 291.1139; Found, 291.1136; The enantiomeric excess of (*R*)-ethyl 1-(4-fluorophenyl)-5-oxo-1,5,6,7-tetrahydropyrazolo[1,2-a]pyrazole-2-carboxylate was determined by chiral stationary-phase HPLC analysis [DAICEL CHIRALPAK AD-H, *i*-PrOH/hexane 20/80, flow rate 1.0 mL/min, t_R .8.1 min (major, 94.3%) and 10.3 min (minor, 5.7%), detection at 330 nm]; $[\alpha]_D^{24}$ −317 (*c* 0.52, $CHCl_3$).

(R)-ethyl 1-(4-iodophenyl)-5-oxo-1,5,6,7-tetrahydropyrazolo[1,2-a]pyrazole-2-carboxylate

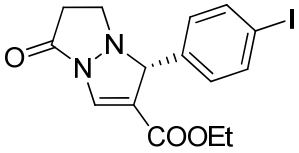

Yellow oil; FTIR (neat) 3084, 2981, 2925, 2851, 1696, 1604, 1509, 1434, 1364, 1319, 1250, 1171, 1105, 1026, 849 cm^{-1}; ^1H NMR (400 MHz, $CDCl_3$) δ 7.53-7.52 (m, 1H), 7.40-7.36 (m, 2H), 7.09-7.03 (m, 2H), 5.14 (d, *J* =1.6 Hz, 1H), 4.13-4.01 (m, 2H) 3.46-3.41 (m, 1H), 3.08-3.01 (m, 1H), 2.97-2.90 (m, 1H), 2.79-2.72 (m, 1H), 1.15 (t, *J* =7.2, 3H); ^{13}C NMR (100 MHz, $CDCl_3$) δ 164.6, 163.3, 134.4, 129.86, 129.79, 128.5, 118.1, 115.5, 115.3, 72.8, 60.4, 51.8, 35.6, 14.0; The enantiomeric excess of (*R*)-ethyl 1-(4-iodophenyl)-5-oxo-1,5,6,7-tetrahydropyrazolo[1,2-a]pyrazole-2-carboxylate was determined by chiral stationary-phase HPLC analysis [DAICEL CHIRALPAK AD-H, *i*-PrOH/hexane 20/80, flow rate 1.0 mL/min, t_R 9.4 min (major, 97%) and 13.2 min (minor, 3%), detection at 330 nm]; $[\alpha]_D^{24}$ −311 (*c* 0.51, $CHCl_3$).

(R)-ethyl1-(4-methoxyphenyl)-5-oxo-1,5,6,7-tetrahydropyrazolo[1,2-a]pyrazole-2-carboxylate

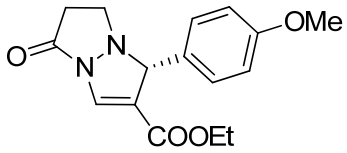

Yellow oil; FTIR (neat) 2929, 2849, 1698, 1603, 1513, 1435, 1365, 1320, 1249, 1197, 1173, 1102, 733 cm^{-1}; ^1H NMR (400 MHz, $CDCl_3$) δ 7.53 (s, 1H), 7.29 (d, *J*=8.8, 2H), 6.90 (d, *J*=8.8, 2H), 5.13 (s, 1H), 4.13-4.03 (m, 2H), 3.80 (s, 3H), 3.36 (m, 1H), 3.03-2.99 (m, 1H), 2.88-2.79 (m, 2H), 1.15 (t, *J*=7.3 Hz, 3H); ^{13}C NMR (125 MHz, CDCl3) δ 164.6 163.4, 159.6, 130.1, 129.3, 128.2, 118.6, 113.9, 72.5, 60.3, 55.2, 51.1, 35.7, 14.0; HRMS (ESI) Calcd for $C_{16}H_{18}N_2O_4^+$ $[M + H]^+$: 303.1139; Found, 303.1336; The enantiomeric excess of (*R*)-ethyl 1-(4-methoxyphenyl)-5-oxo-1,5,6,7-tetrahydropyrazolo[1,2-a]pyrazole-2-carboxylate was determined by chiral stationary-phase HPLC analysis [DAICEL CHIRALPAK AD-H, *i*-PrOH/hexane 20/80, flow rate 1.0 mL/min, t_R .11.1 min (major, 92%) and 11.6 min (minor, 8%), detection at 330 nm]; $[\alpha]_D^{23}$ −346 (*c* 0.51, $CHCl_3$).

(R)-methyl 5-oxo-1-phenyl-1,5,6,7-tetrahydropyrazolo[1,2-a]pyrazole-2-carboxylate

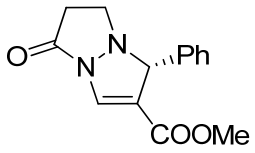

Yellow solid; FTIR (neat) 3083, 2921, 2862, 1714, 1604, 1456, 1407, 1305, 1246, 1210, 1167, 1105, 700 cm^{-1}; ^{1}H NMR (400 MHz, $CDCl_3$) δ 7.53 (brs, 1H), 7.38-7.31 (m, 5H), 5.17 (d, *J* =1.6 Hz, 1H), 3.62 (s, 3H), 3.41-3.36 (m, 1H), 3.08-3.01 (m, 1H), 2.94-2.85 (m, 1H), 2.79-2.72 (m, 1H); ^{13}C NMR (100 MHz, $CDCl_3$) δ 164.7, 163.8, 138.1, 128.6, 128.5, 128.2, 117.9, 73.1, 51.5, 35.7; HRMS (ESI) Calcd for $C_{14}H_{15}N_2O_3^+$ $[M + H]^+$: 259.1077; Found, 259.1073; The enantiomeric excess of (*R*)-methyl 5-oxo-1-phenyl-1,5,6,7-tetrahydropyrazolo[1,2-a]pyrazole-2-carboxylate was determined by chiral stationary-phase HPLC analysis [DAICEL CHIRALPAK AD-H, *i*-PrOH/hexane 20/80, flow rate 1.0 mL/min, t_R 11.3 min (major, 99%) and 12.7 min (minor, 1%), detection at 330 nm]; $[\alpha]_D^{24}$ −446 (*c* 0.91, $CHCl_3$).

(R)-tert-butyl
5-oxo-1-phenyl-1,5,6,7-tetrahydropyrazolo[1,2-a]pyrazole-2-carboxylate

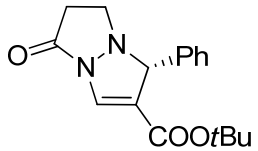

Yellow oil; FTIR (neat) 3084, 2977, 2929, 2850, 1695, 1602, 1435, 1367, 1306, 1253, 1156, 1109, 843, 751, 699 cm^{-1}; ^{1}H NMR (400 MHz, $CDCl_3$) δ 7.49 (brs, 1H), 7.39–7.32 (m, 5H), 5.09 (d, *J*=1.6 Hz, 1H), 3.42-3.37 (m, 1H), 3.08–3.01 (m, 1H), 2.93-2.84 (m, 1H), 2.78–2.71 (m, 1H), 1.29 (s, 9H); ^{13}C NMR (100 MHz, $CDCl_3$) δ 164.4, 162.7, 138.6, 128.5, 128.3, 128,2, 128.1, 120.3, 81.1, 73.6, 51.7, 35.7, 27.9; HRMS (ESI) Calcd for $C_{17}H_{21}N_2O_3^+$ $[M + H]^+$: 301.1547; Found, 301.1541; The enantiomeric excess of (*R*)-tert-butyl-5-oxo-1-phenyl-1,5,6,7-tetrahydropyrazolo[1,2-a]pyrazole-2-carboxylate was determined by chiral stationary-phase HPLC analysis [DAICEL CHIRALPAK OD-H, *i*-PrOH/hexane 20/80, flow rate 1.0 mL/min, t_R 9.2 min (major, 90%) and 11.6 min (minor, 10%), detection at 330 nm]; $[\alpha]_D^{24}$ −237 (*c* 0.56, $CHCl_3$).

(R)-ethyl 1-cyclohexyl-5-oxo-1,5,6,7-tetrahydropyrazolo[1,2-a]pyrazole-2-carboxylate

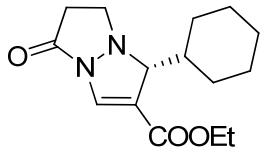

Yellow solid; FTIR (neat) 3115, 2981, 2923, 2852, 1696, 1605, 1482, 1360, 1365, 1255, 1205, 1021, 964, 754 cm^{-1}; ^{1}H NMR (400 MHz, CDCl3) δ 7.38 (s, 1H), 4.26-4.14 (m, 2H), 4.05 (s, 1H), 3.60-3.56 (m, 1H), 2.99-2.90 (m, 2H), 2.62-2.58 (m, 1H), 2.02-1.12 (m, 14H); ^{13}C NMR (100 MHz, $CDCl_3$) δ 166.4 164.0, 129.6, 115.7, 75.7, 60.3, 56.1, 39.2, 35.0, 30.1, 26.7, 26.5, 26.3, 25.9, 14.2; HRMS (ESI) Calcd for $C_{15}H_{22}N_2O_3^+$ $[M+H]^+$: 279.1730; Found, 279.1700; The enantiomeric excess of (*R*)-ethyl 1-cyclohexyl-5-oxo-1,5,6,7-tetrahydropyrazolo[1,2-a]pyrazole-2-carboxylate was determined by chiral stationary-phase HPLC analysis [DAICEL CHIRALPAK OJ-H, *i*-PrOH/hexane 20/80, flow rate 1.0 mL/min, *t*R .5.6 min (major, 94%) and 7.1 min (minor, 6%), detection at 330 nm]; $[\alpha]_D^{24}$ −440 (*c* 0.47, CHCl3).

(R)-ethyl 1-isopropyl-5-oxo-1,5,6,7-tetrahydropyrazolo[1,2-a]pyrazole-2-carboxylate

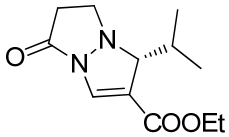

Yellow oil; FTIR (neat) 2963, 2933, 2873, 1694, 1602, 1541, 1415, 1362, 1313, 1255, 1195, 1169, 1103, 1023, 784, 662 cm^{-1}; ^{1}H NMR (400 MHz, $CDCl_3$) δ 7.40 (s, 1H), 4.31-4.13 (m, 2H), 4.10-4.09 (m, 1H), 3.63-3.53 (m, 1H) 3.03-2.93 (m, 2H), 2.66-2.57 (m, 1H), 2.36 (sepd, J = 6.8, 2.7 Hz, 1H), 1.29 (t, J = 7.1 Hz, 3H), 0.96 (t, J = 6.8 Hz, 3H), 0.85 (t, J = 6.8 Hz, 3H); ^{13}C NMR (100 MHz, $CDCl_3$) δ 166.5, 164.0, 129.8, 116.3, 76.0, 60.4, 56.1, 35.1, 29.2, 19.5, 16.1, 14.2; HRMS (ESI) Calcd for $C_{12}H_{18}N_2O_3Na^+$ $[M+Na]^+$: 261.1210; Found, 261.1208; The enantiomeric excess was determined by chiral stationary-phase HPLC analysis [DAICEL CHIRALPAK OJ-H, i-PrOH/hexane 10/90, flow rate 1.0 mL/min, tR 7.3 min (major, 92.4%) and 11.8 min (minor, 7.6%), detection at 330 nm]; $[\alpha]_D^{20}$ −566 (*c* = 0.23, $CHCl_3$).

6. ^{1}H-NMR and ^{13}C-NMR spectra of Compounds (A-E) toward the solid-phase catalysis

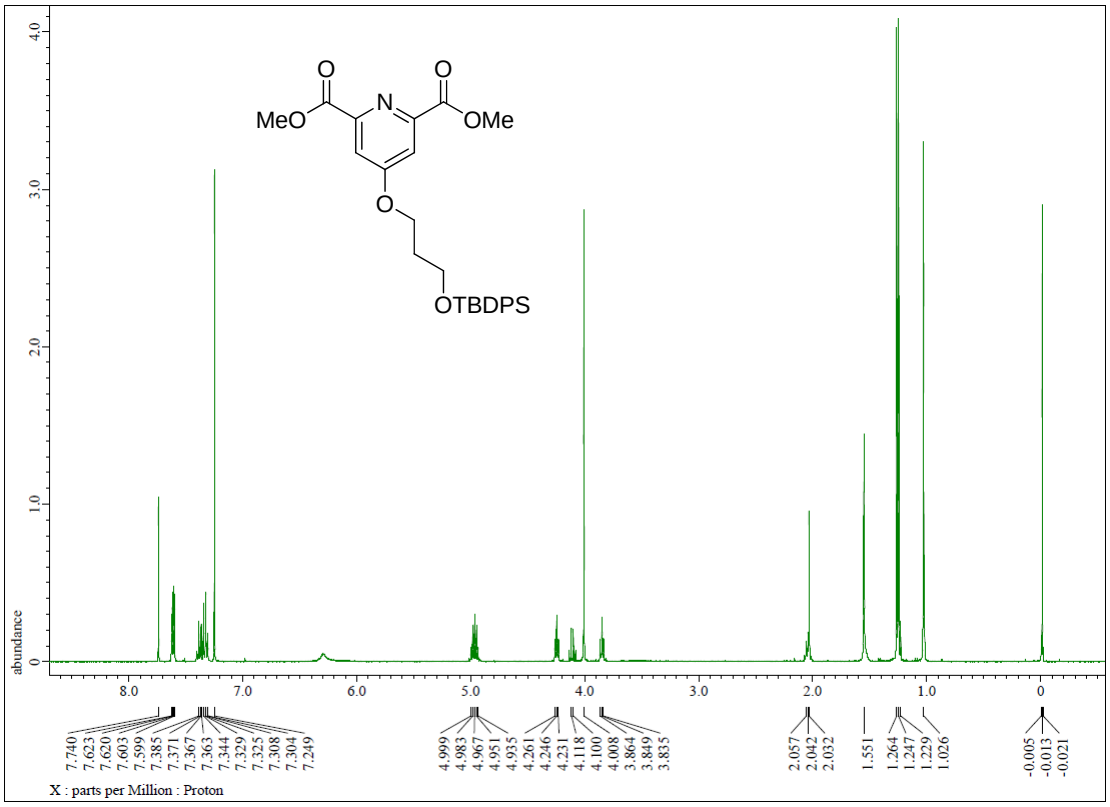

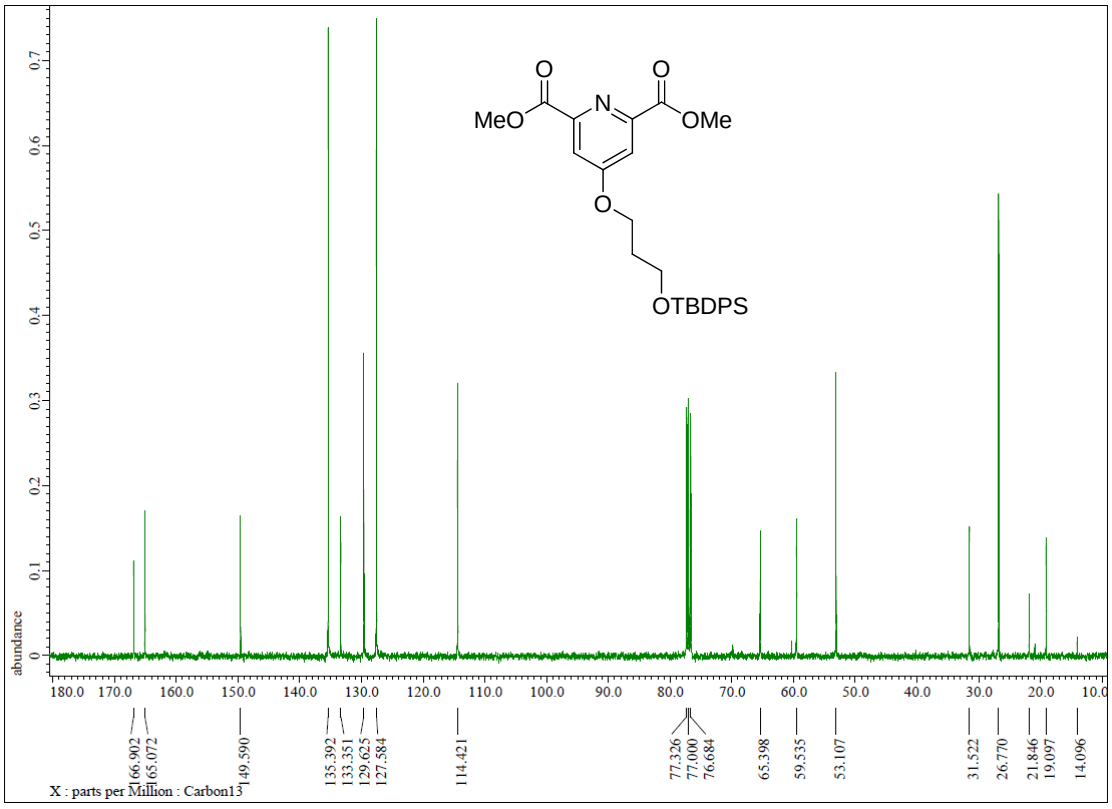

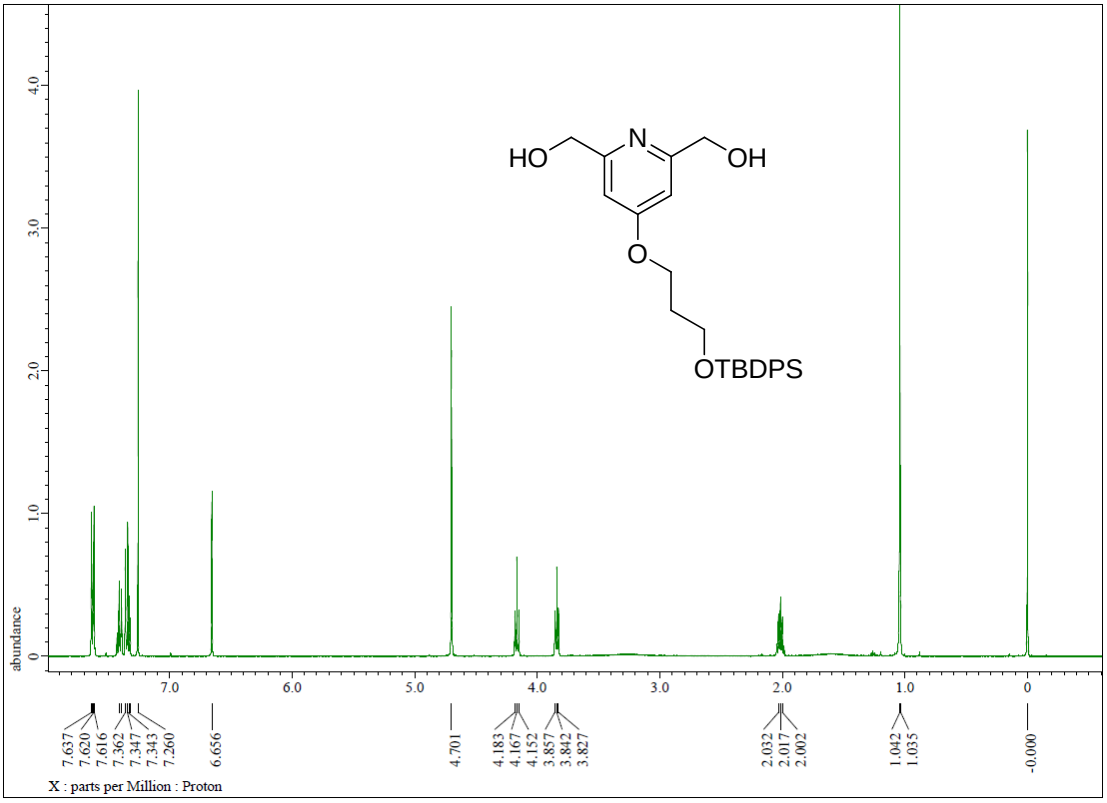
HO
N
OH
O
OTBDPS
abundance
7.637
7.620
7.616
7.362
7.347
7.343
7.260
6.656
4.701
4.183
4.167
4.152
3.857
3.842
3.827
2.032
2.017
2.002
1.042
1.035
-0.000
X : parts per Million : Proton

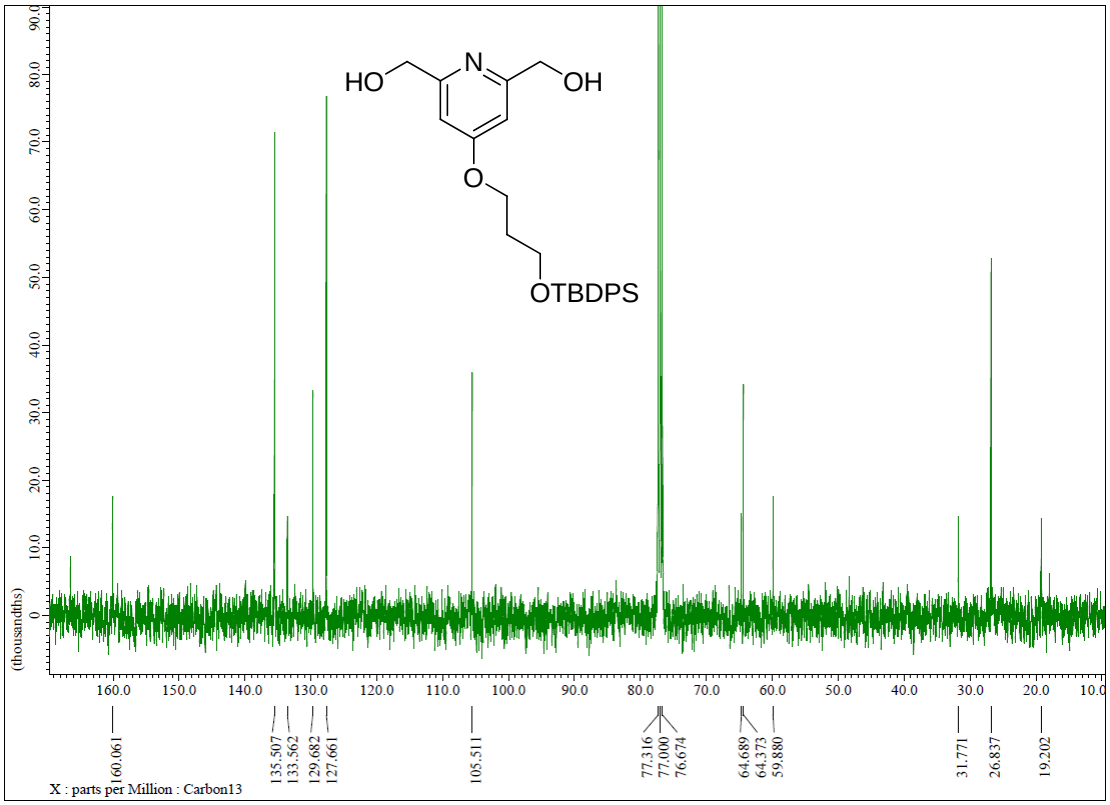
HO
N
OH
O
OTBDPS
(thousandths)
160.061
135.507
133.562
129.682
127.661
105.511
77.316
77.000
76.674
64.689
64.373
59.880
31.771
26.837
19.202
X : parts per Million : Carbon13

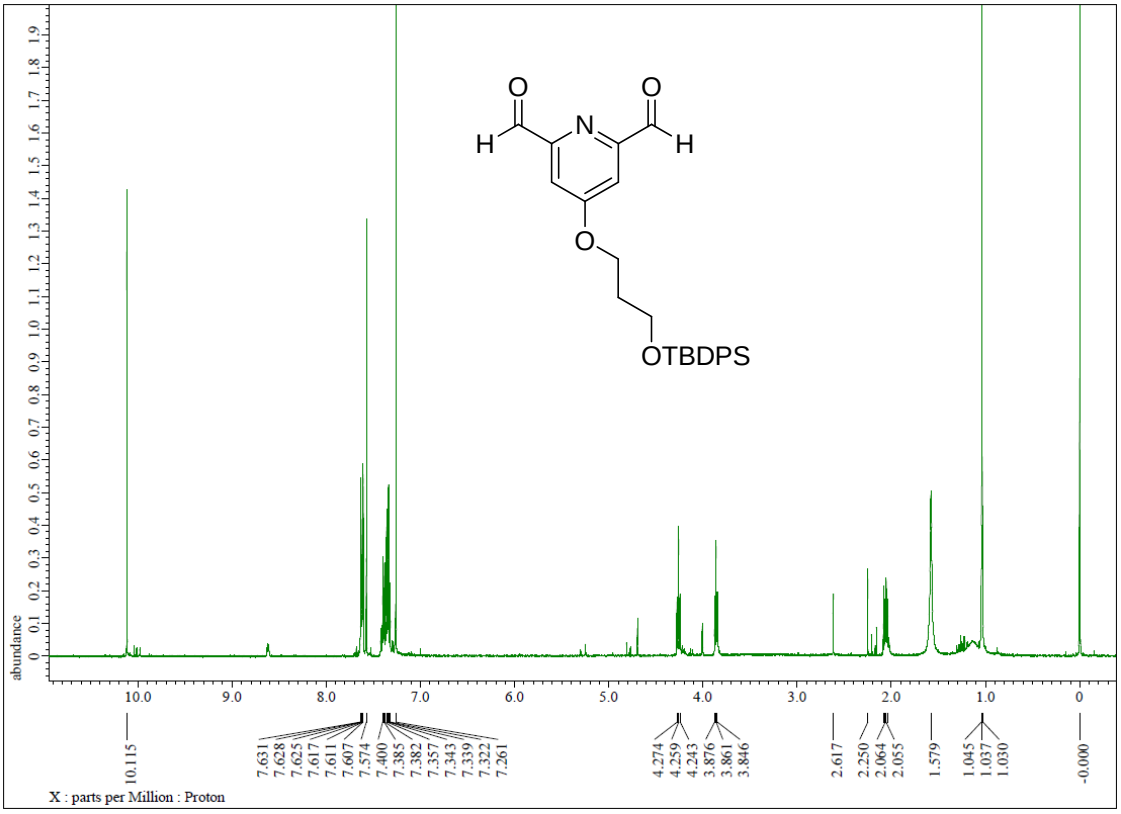
O
O
H
N
H
O
OTBDPS
abundance
10.115
7.631
7.628
7.625
7.617
7.611
7.607
7.574
7.400
7.385
7.382
7.357
7.343
7.339
7.322
7.261
4.274
4.259
4.243
3.876
3.861
3.846
2.617
2.250
2.064
2.055
1.579
1.045
1.037
1.030
-0.000
X : parts per Million : Proton

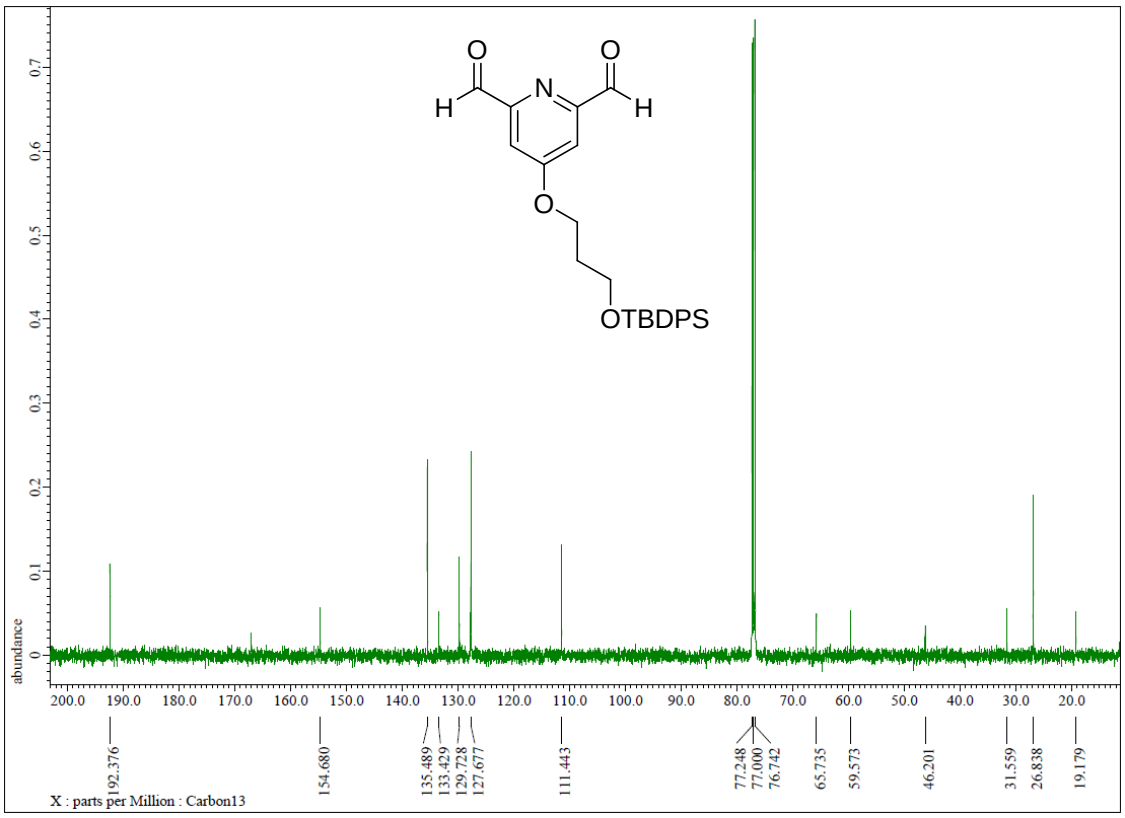
O
O
H
N
H
O
OTBDPS
abundance
192.376
154.680
135.489
133.429
129.728
127.677
111.443
77.248
77.000
76.742
65.735
59.573
46.201
31.559
26.838
19.179
X : parts per Million : Carbon13

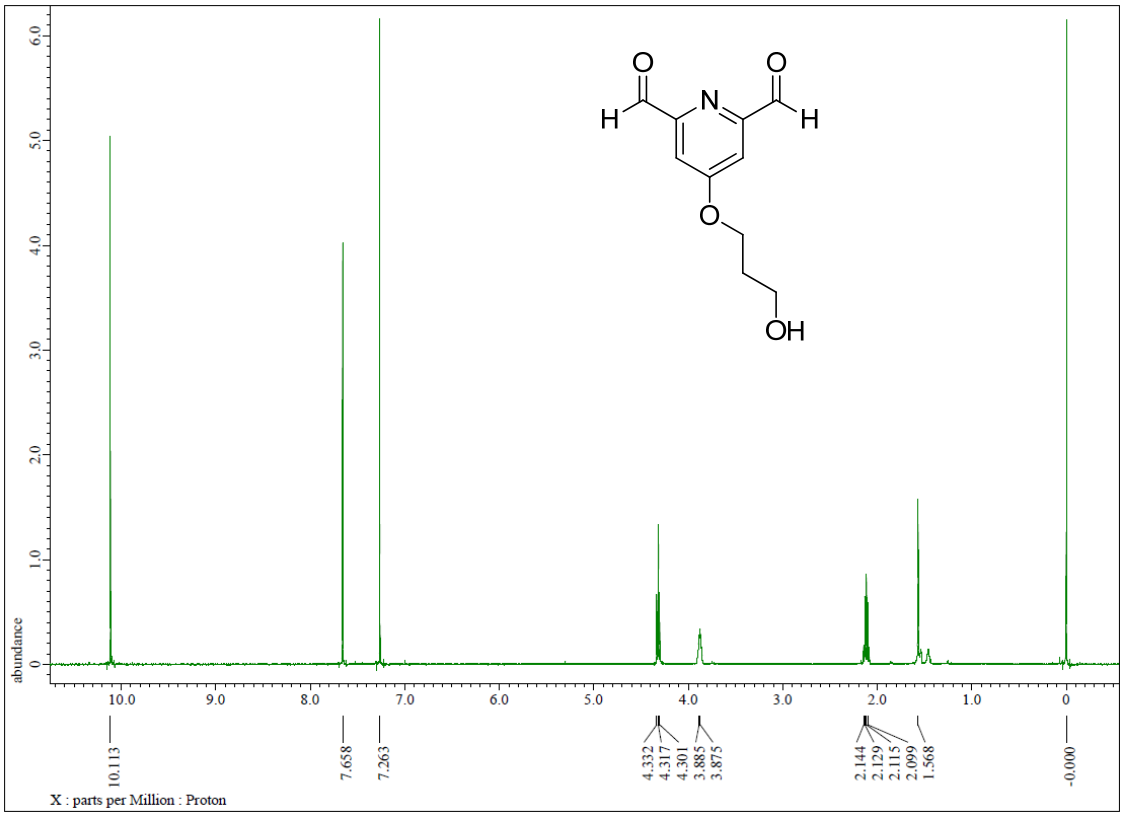
O
O
H
N
H
O
OH
abundance
X : parts per Million : Proton
10.113
7.658
7.263
4.332
4.317
4.301
3.885
3.875
2.144
2.129
2.115
2.099
1.568
-0.000

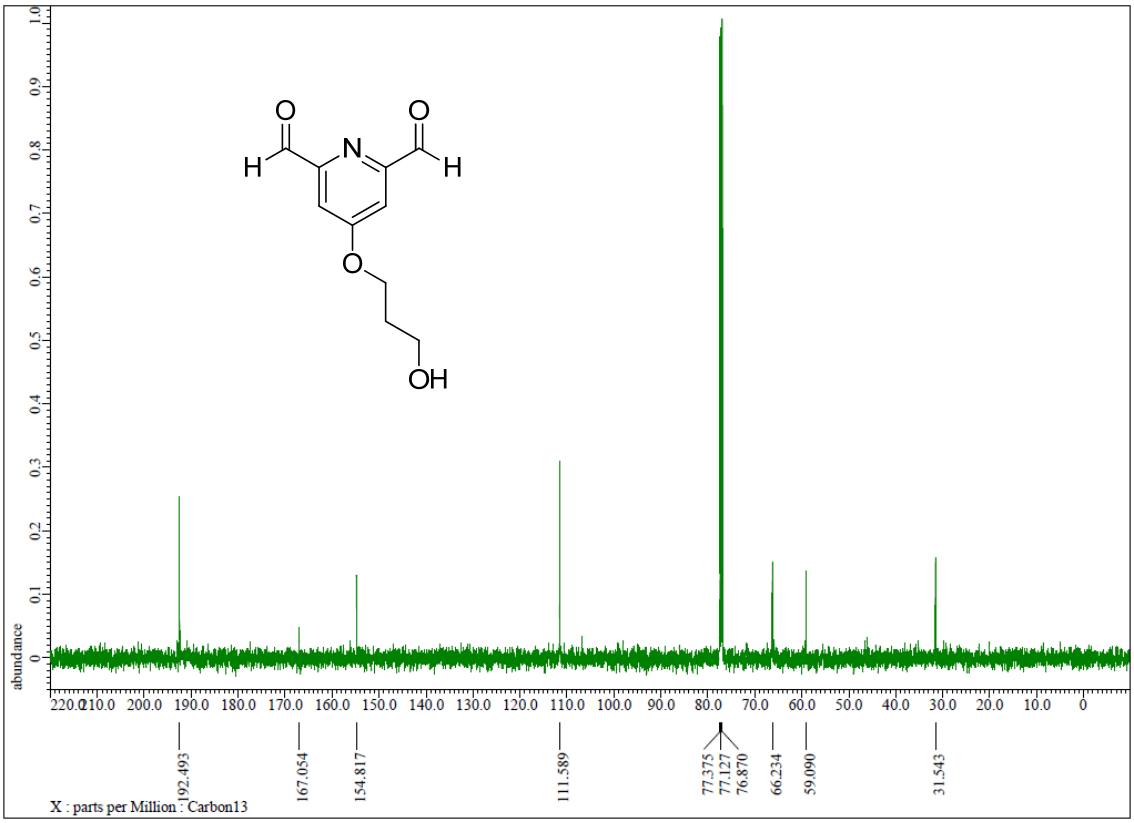
O
O
H
N
H
O
OH
abundance
X : parts per Million : Carbon13
192.493
167.054
154.817
111.589
77.375
77.127
76.870
66.234
59.090
31.543

7. ^{1}H-NMR and ^{13}C-NMR spectra of PyBodines

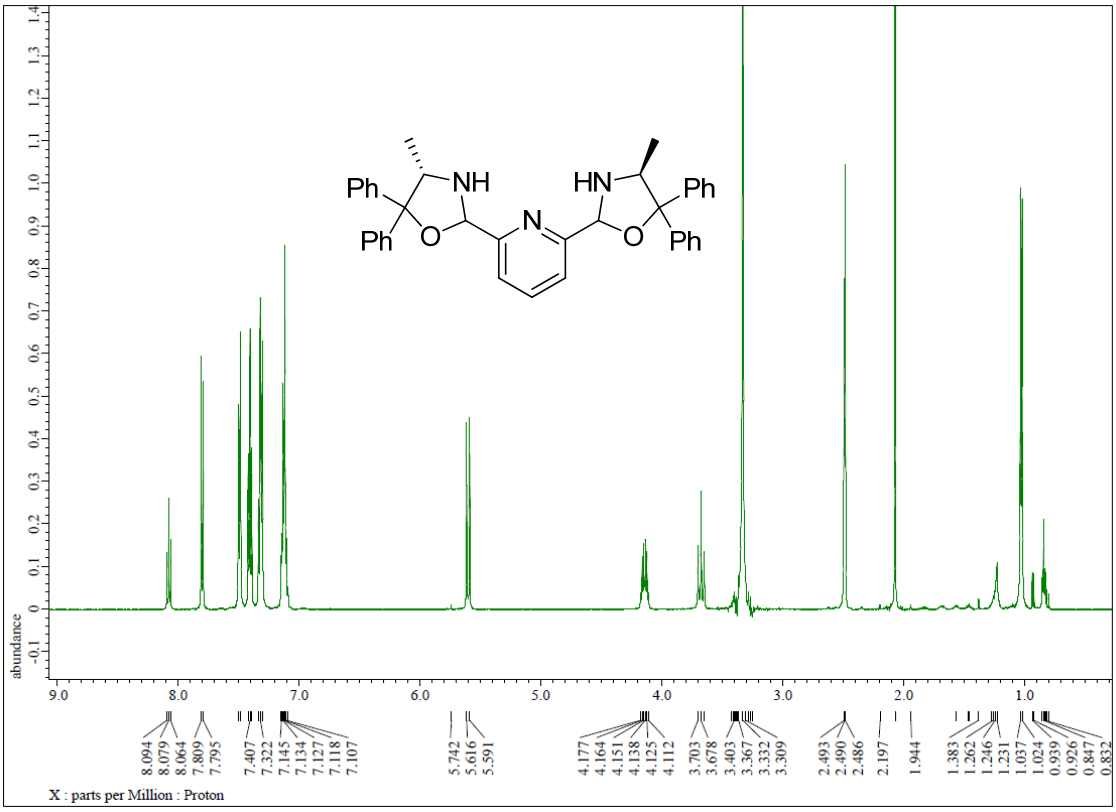

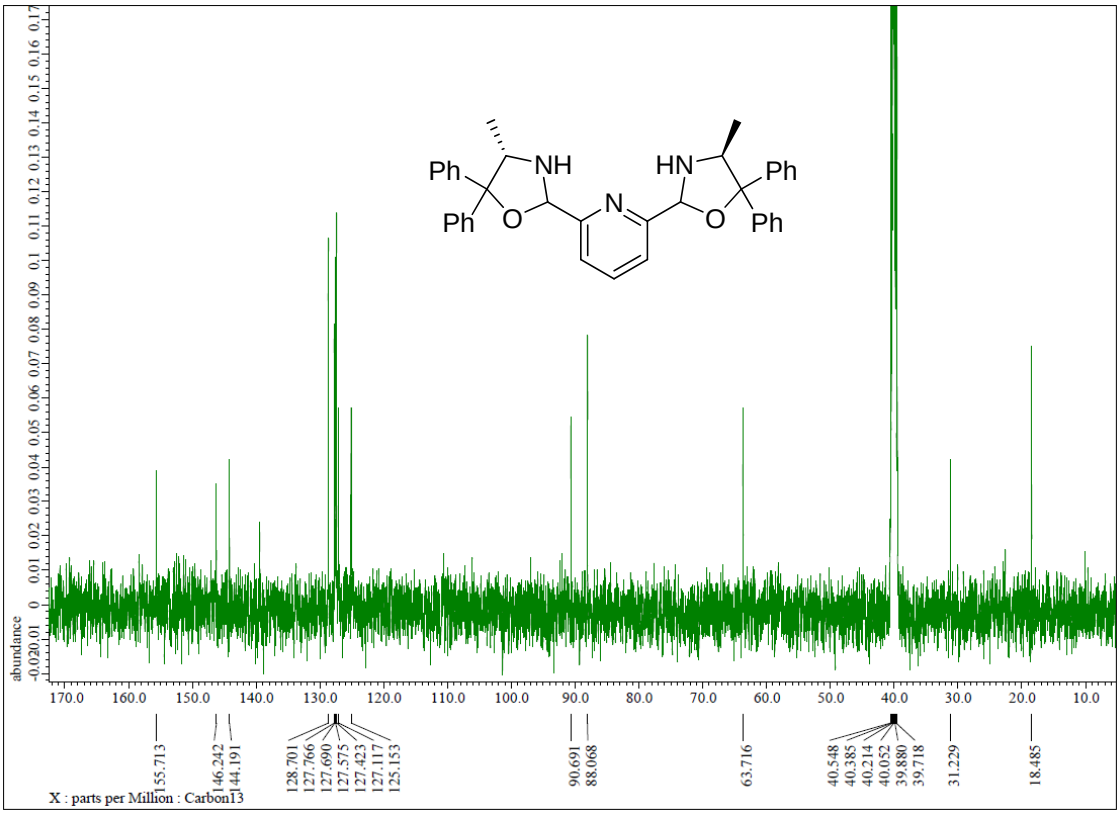

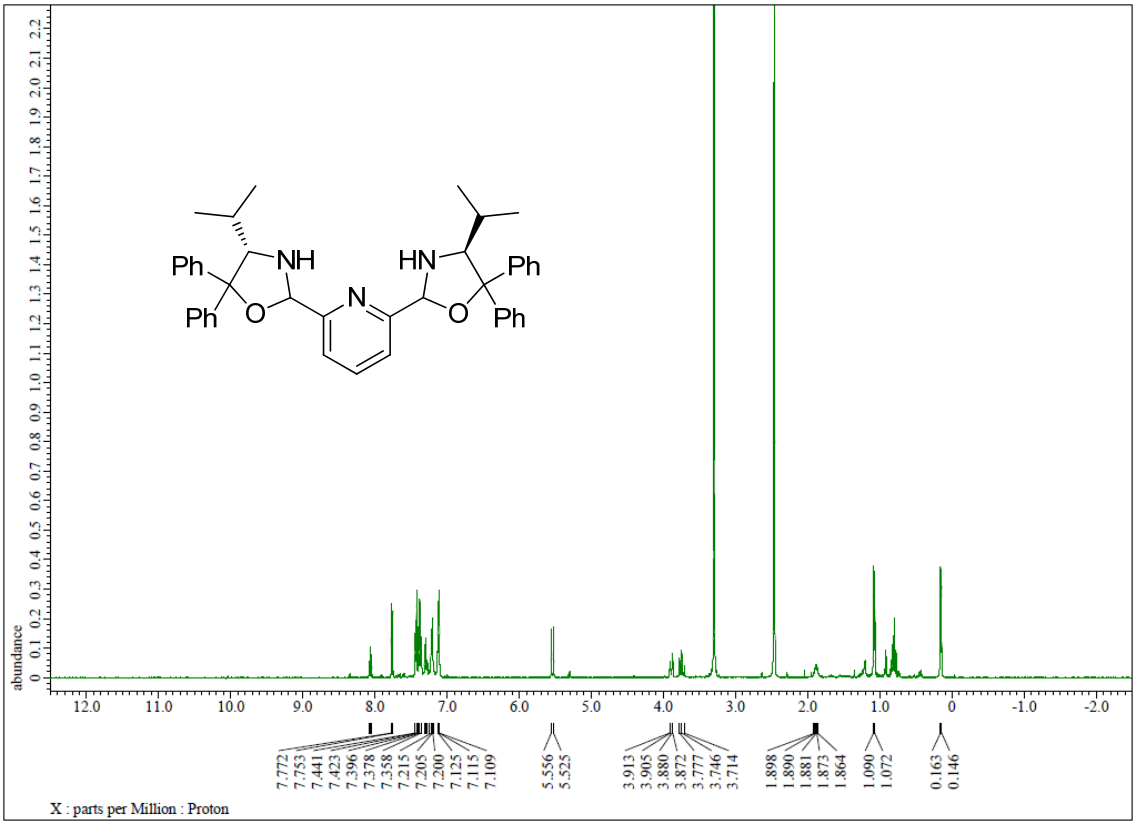
Ph
NH
HN
Ph
Ph
O
N
O
Ph
abundance
X : parts per Million : Proton
7.772
7.753
7.441
7.423
7.396
7.378
7.358
7.215
7.205
7.200
7.125
7.115
7.109
5.556
5.525
3.913
3.905
3.880
3.872
3.777
3.746
3.714
1.898
1.890
1.881
1.873
1.864
1.090
1.072
0.163
0.146

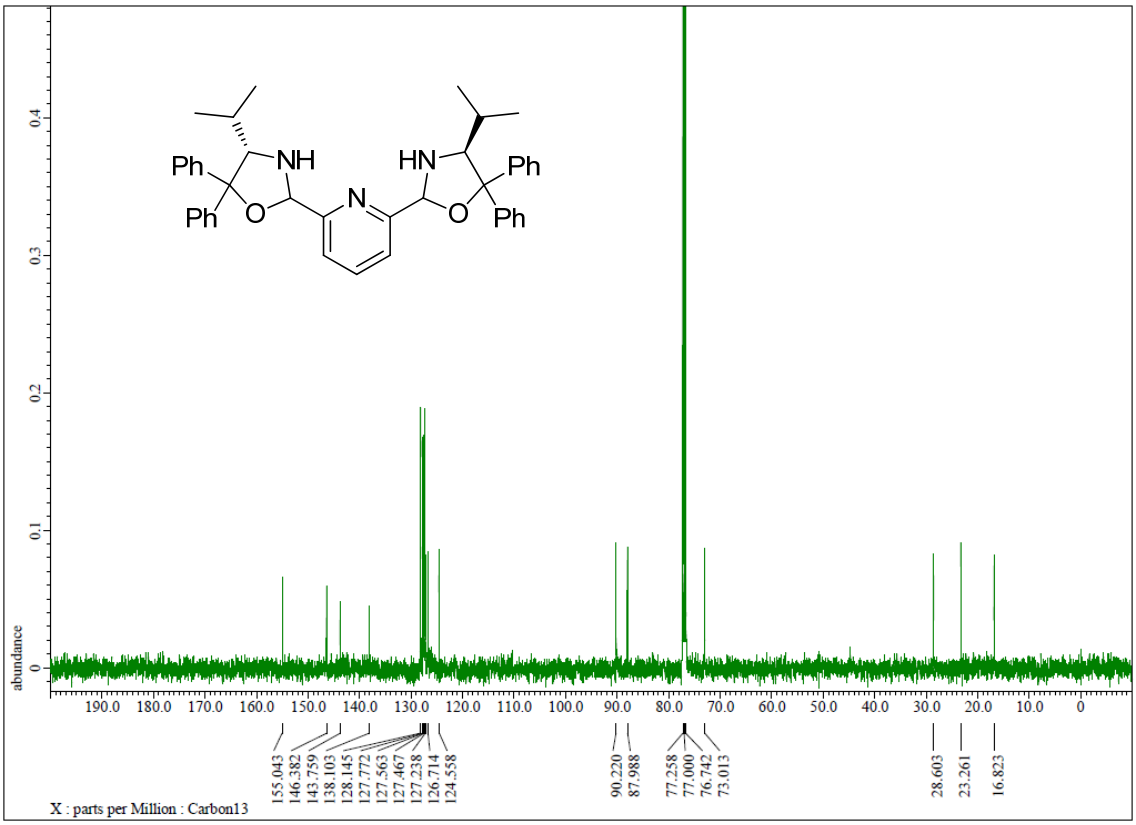
Ph
NH
HN
Ph
Ph
O
N
O
Ph
abundance
X : parts per Million : Carbon13
155.043
146.382
143.759
138.103
128.145
127.772
127.563
127.467
127.238
126.714
124.558
90.220
87.988
77.258
77.000
76.742
73.013
28.603
23.261
16.823

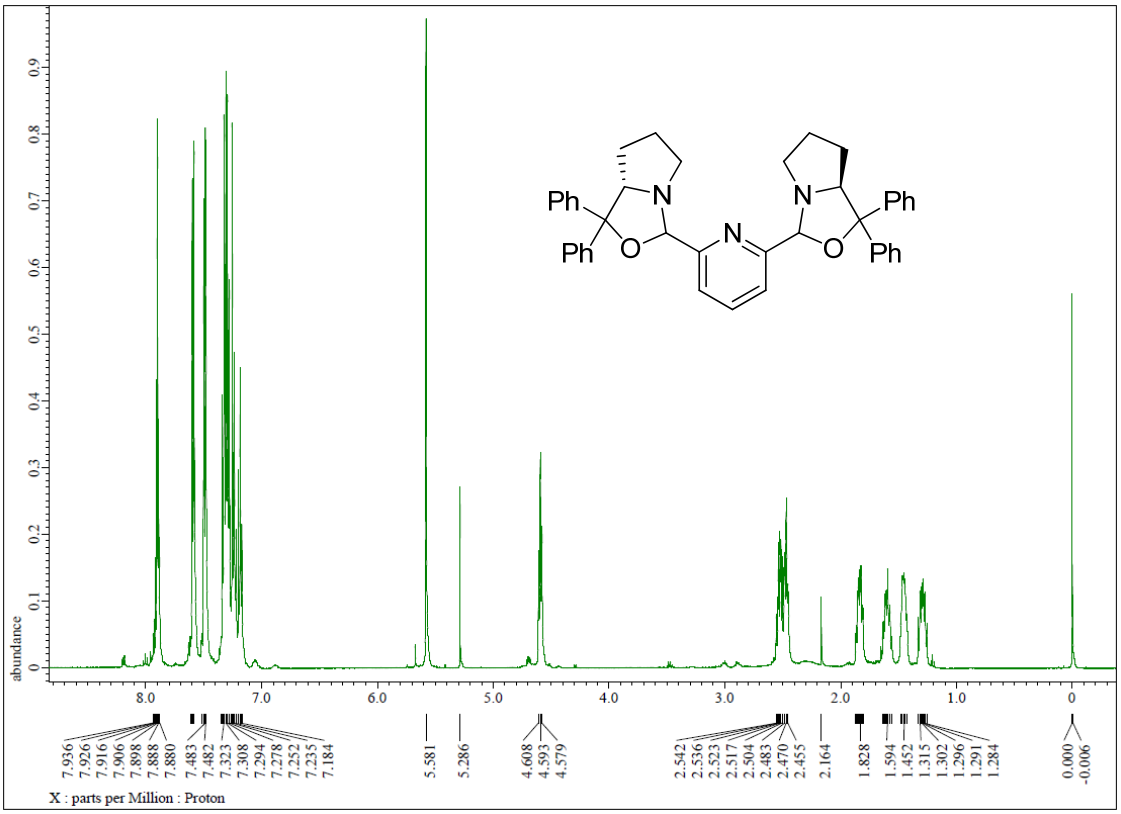
abundance
X : parts per Million : Proton
7.936
7.926
7.916
7.906
7.898
7.888
7.880
7.483
7.482
7.323
7.308
7.294
7.278
7.252
7.235
7.184
5.581
5.286
4.608
4.593
4.579
2.542
2.536
2.523
2.517
2.504
2.483
2.470
2.455
2.164
1.828
1.594
1.452
1.315
1.302
1.296
1.291
1.284
0.000
-0.006

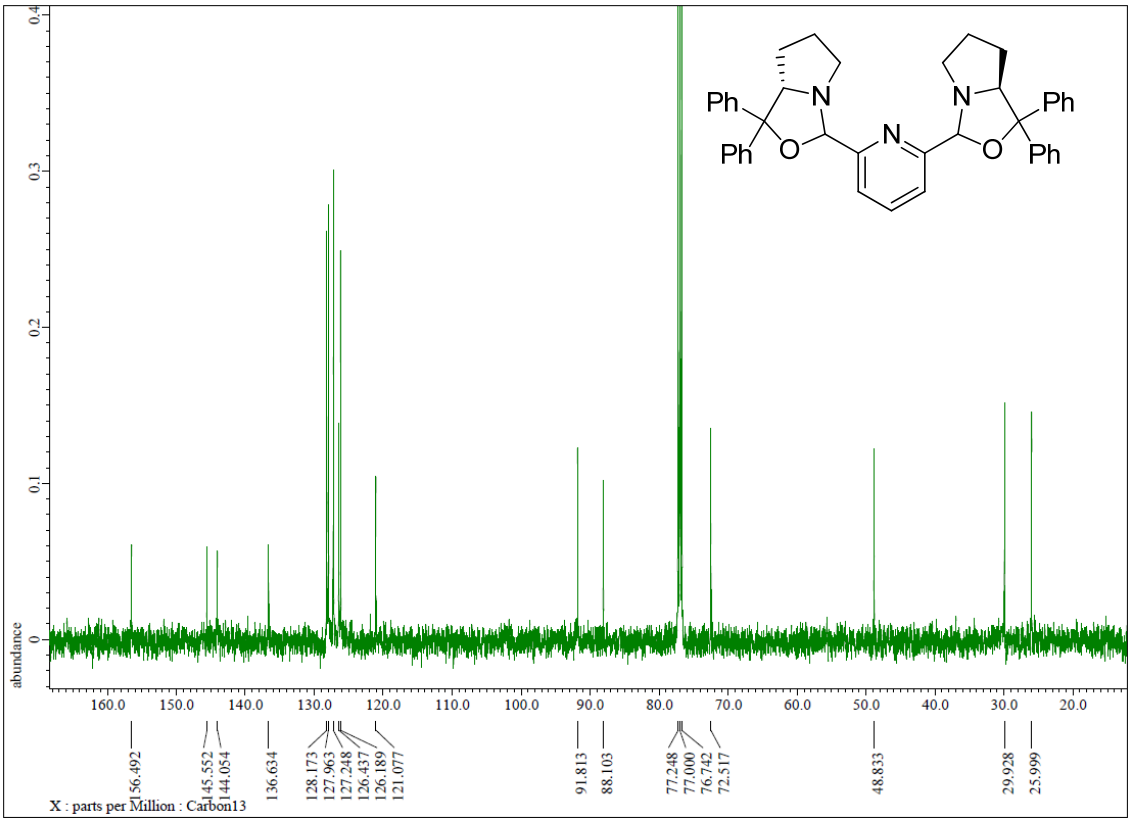
abundance
X : parts per Million : Carbon13
156.492
145.552
144.054
136.634
128.173
127.963
127.248
126.437
126.189
121.077
91.813
88.103
77.248
77.000
76.742
72.517
48.833
29.928
25.999

8. ^{1}H-NMR and ^{13}C-NMR spectra of [3+2]-cycloadducts

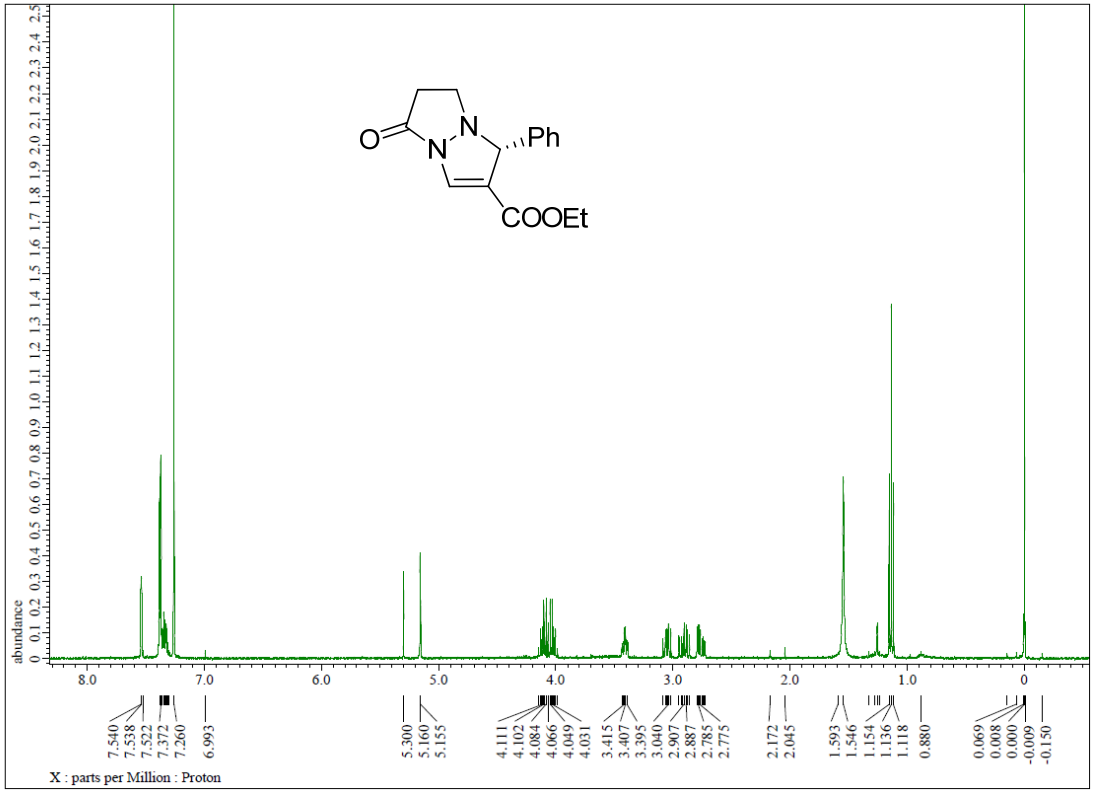

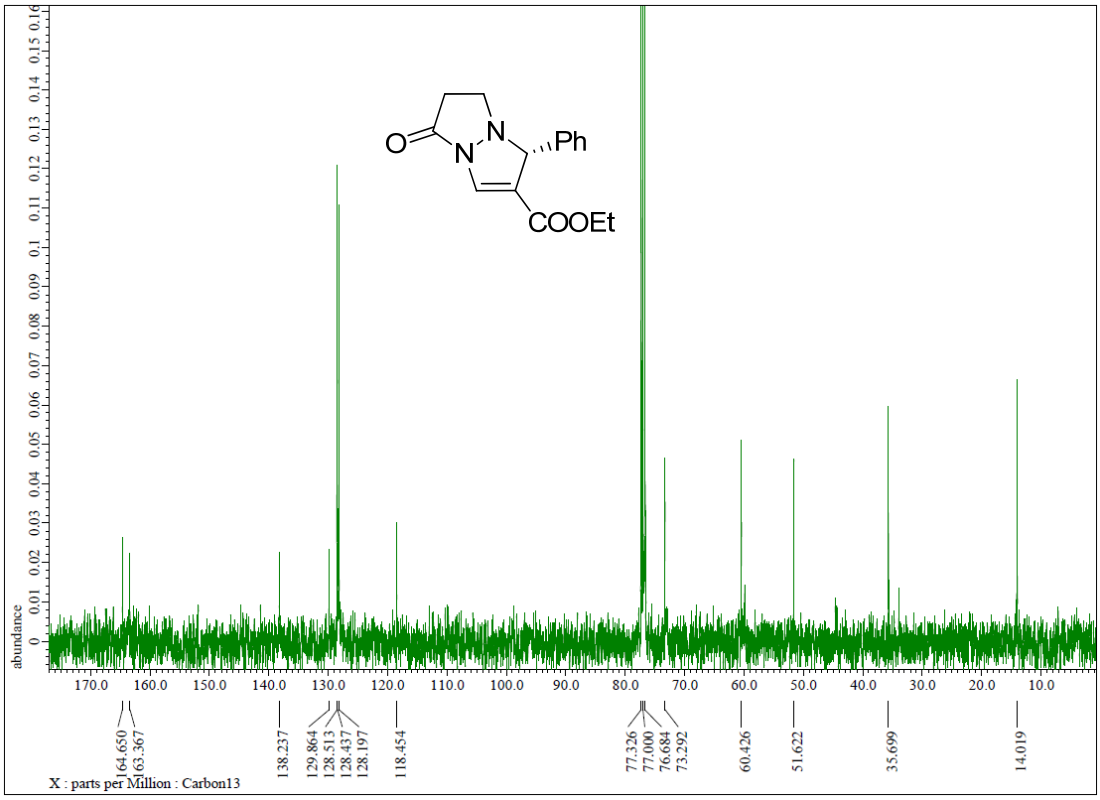

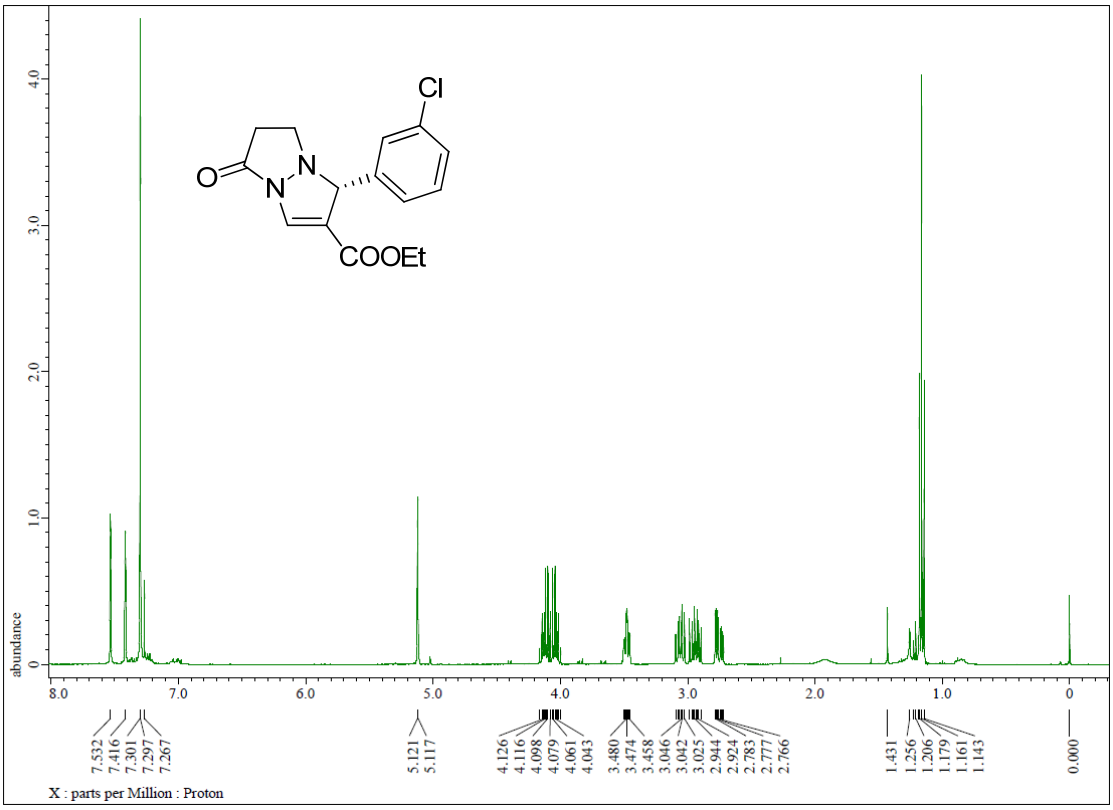
Cl
O
N
N
COOEt
abundance
X : parts per Million : Proton
7.532
7.416
7.301
7.297
7.267
5.121
5.117
4.126
4.116
4.098
4.079
4.061
4.043
3.480
3.474
3.458
3.046
3.042
3.025
2.944
2.924
2.783
2.777
2.766
1.431
1.256
1.206
1.179
1.161
1.143
0.000

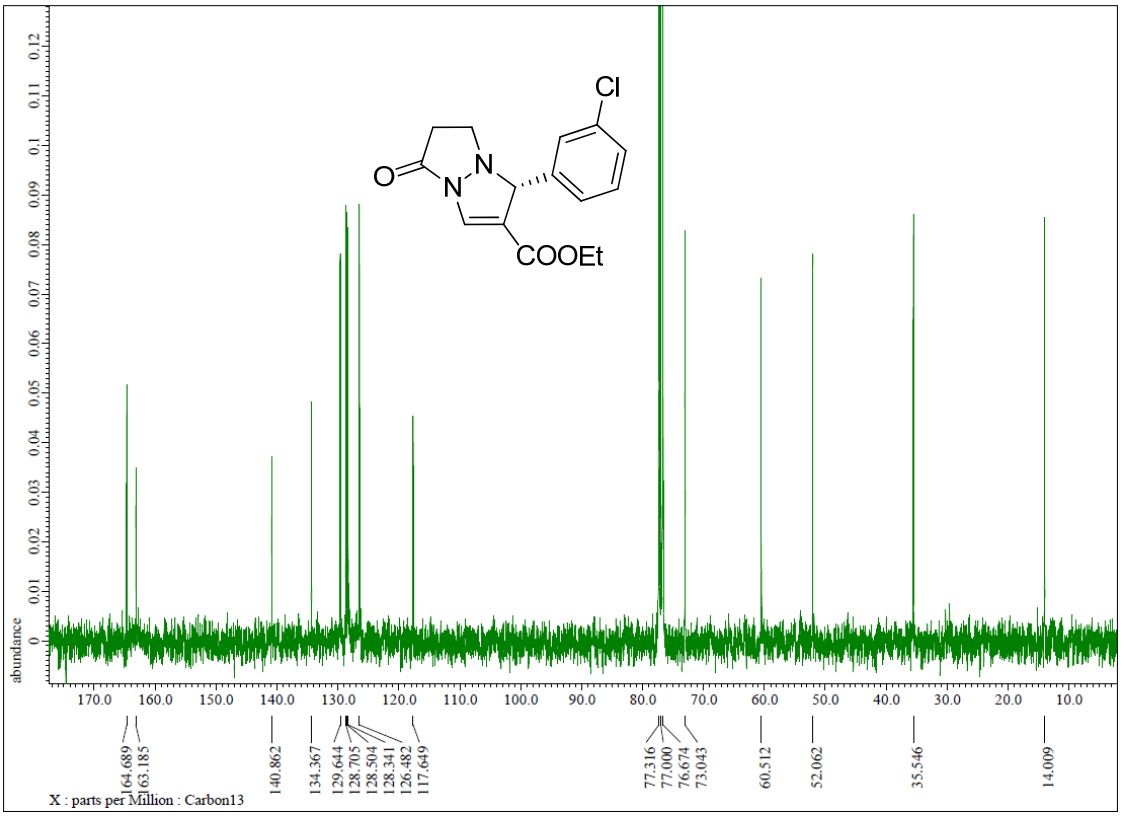
Cl
O
N
N
COOEt
abundance
X : parts per Million : Carbon13
164.689
163.185
140.862
134.367
129.644
128.705
128.504
128.341
126.482
117.649
77.316
77.000
76.674
73.043
60.512
52.062
35.546
14.009

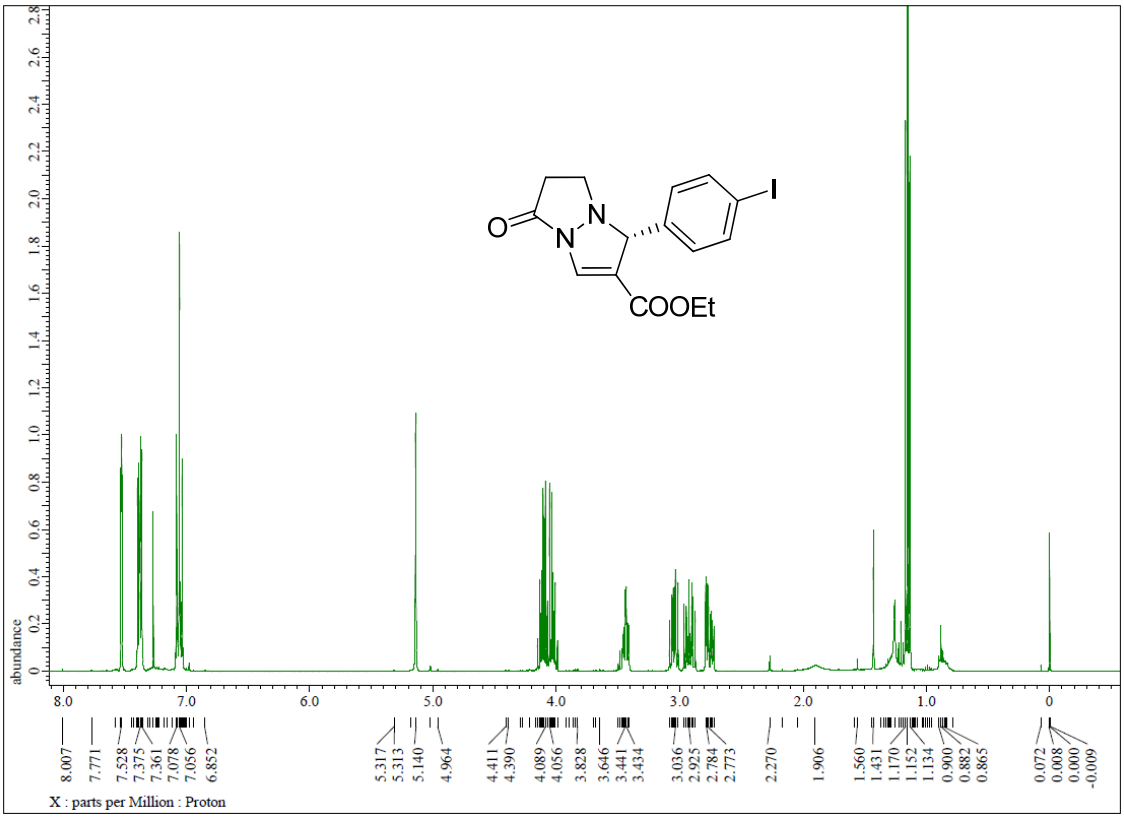
O
N
N
I
COOEt
abundance
X : parts per Million : Proton
8.007
7.771
7.528
7.375
7.361
7.078
7.056
6.852
5.317
5.313
5.140
4.964
4.411
4.390
4.089
4.056
3.828
3.646
3.441
3.434
3.036
2.925
2.784
2.773
2.270
1.906
1.560
1.431
1.170
1.152
1.134
0.900
0.882
0.865
0.072
0.008
0.000
-0.009

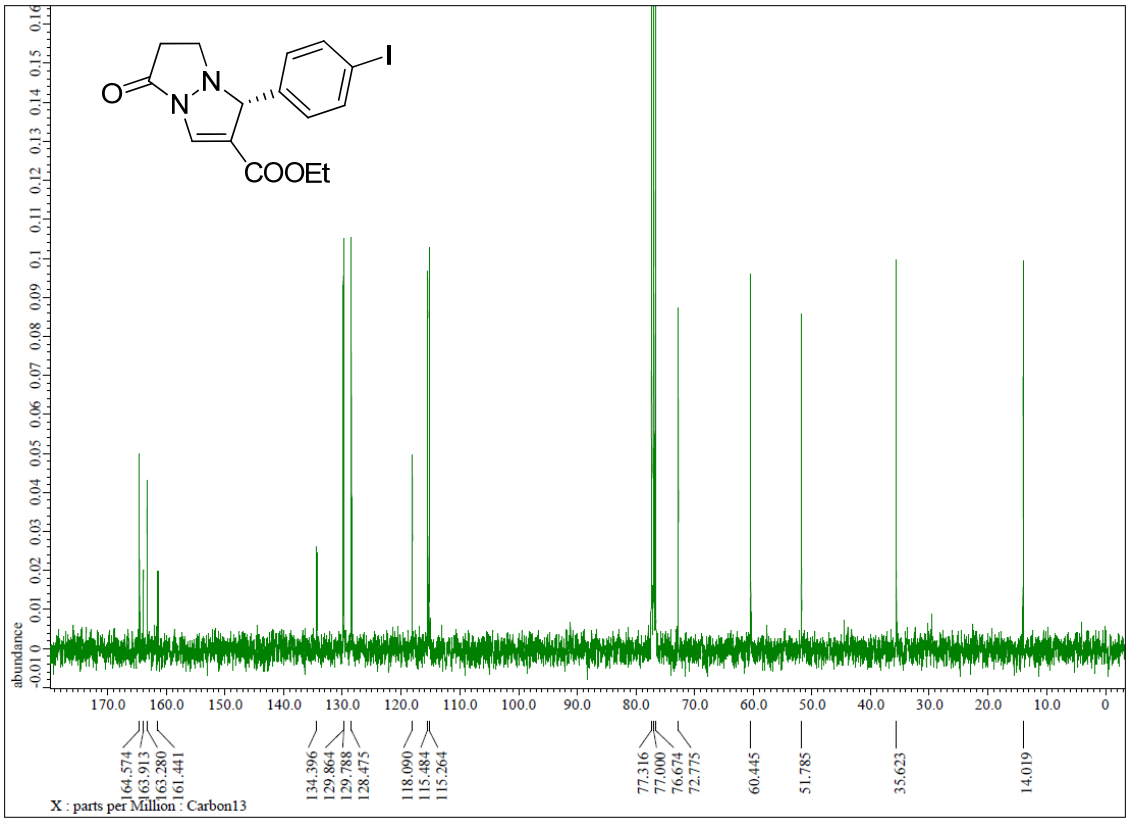
O
N
N
I
COOEt
abundance
X : parts per Million : Carbon13
164.574
163.913
163.280
161.441
134.396
129.864
129.788
128.475
118.090
115.484
115.264
77.316
77.000
76.674
72.775
60.445
51.785
35.623
14.019

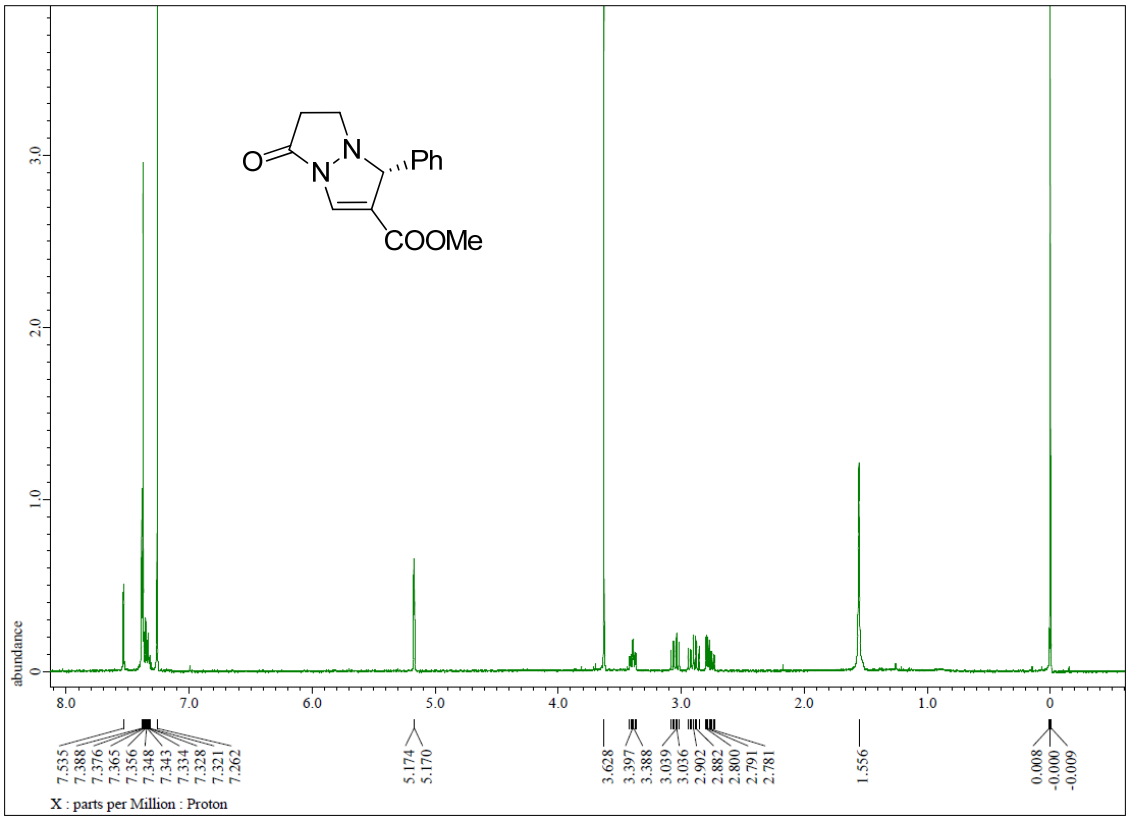
O
N
N
Ph
COOMe
abundance
3.0
2.0
1.0
0
8.0
7.0
6.0
5.0
4.0
3.0
2.0
1.0
0
7.535
7.388
7.376
7.365
7.356
7.348
7.343
7.334
7.328
7.321
7.262
5.174
5.170
3.628
3.397
3.388
3.039
3.036
2.902
2.882
2.800
2.791
2.781
1.556
0.008
-0.000
-0.009
X : parts per Million : Proton

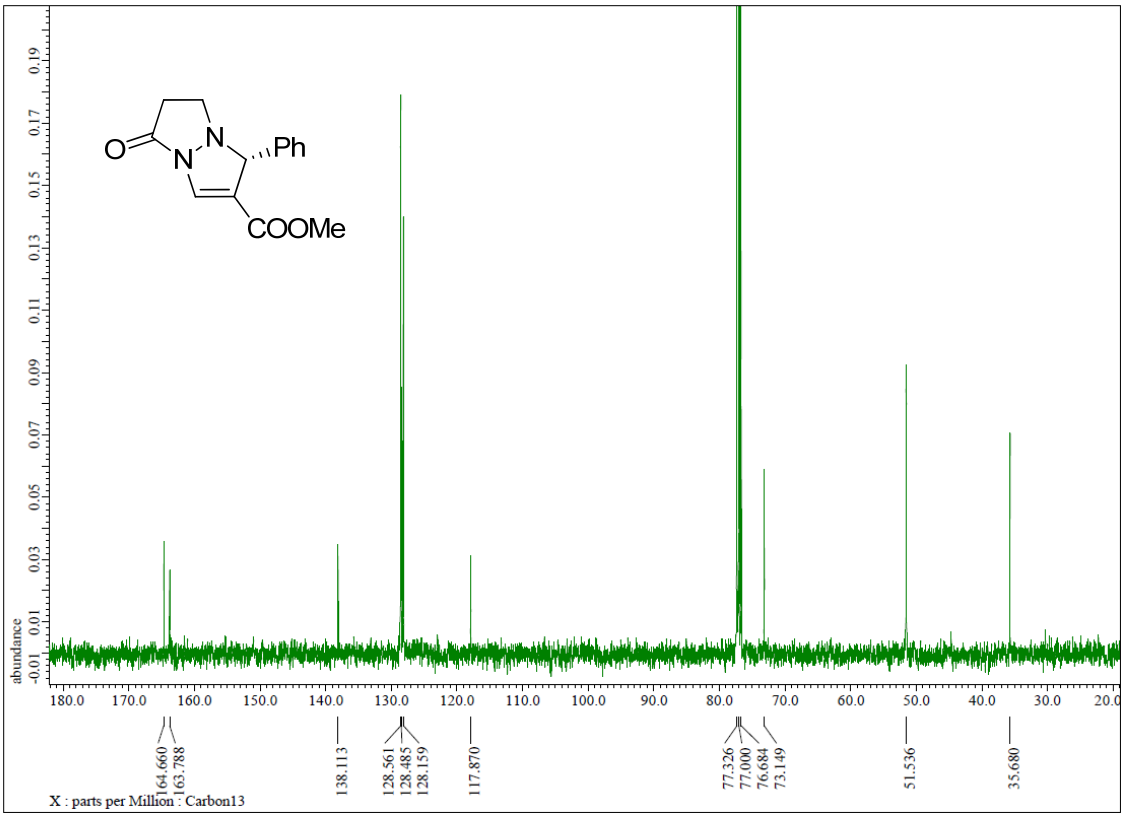
O
N
N
Ph
COOMe
abundance
0.19
0.17
0.15
0.13
0.11
0.09
0.07
0.05
0.03
0.01
-0.01
180.0
170.0
160.0
150.0
140.0
130.0
120.0
110.0
100.0
90.0
80.0
70.0
60.0
50.0
40.0
30.0
164.660
163.788
138.113
128.561
128.485
128.159
117.870
77.326
77.000
76.684
73.149
51.536
35.680
X : parts per Million : Carbon13

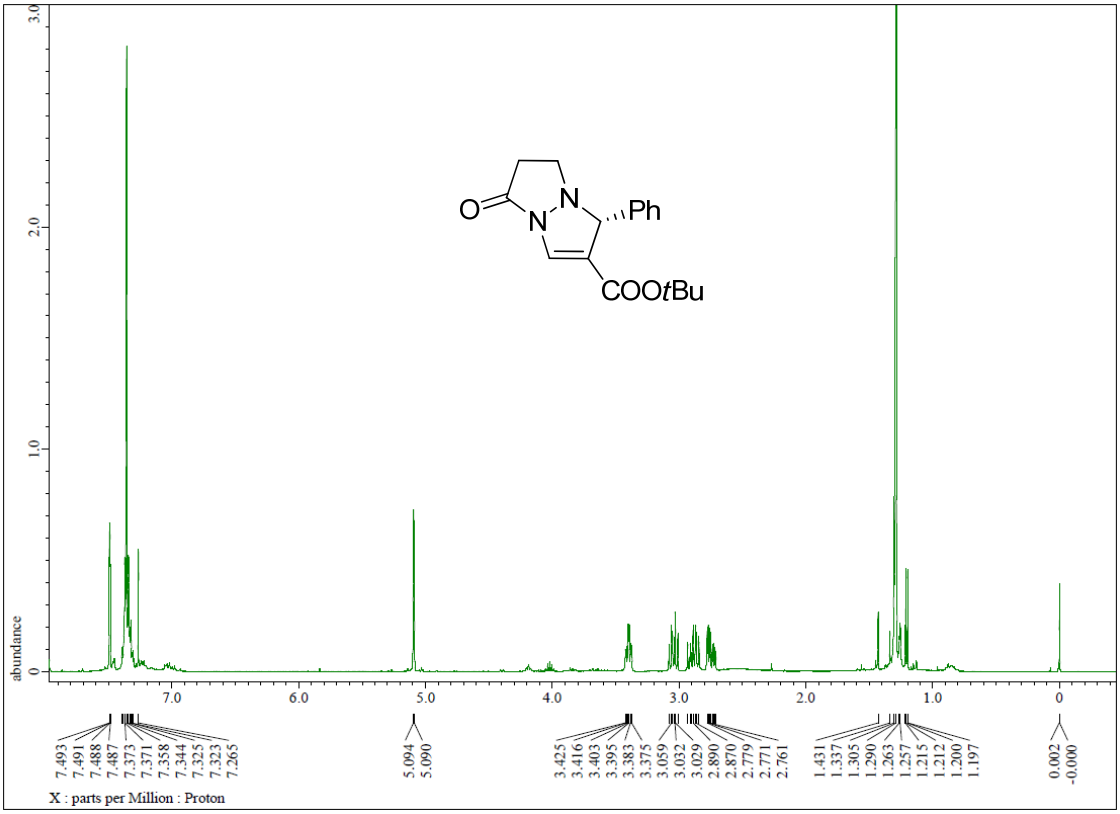
O
N
N
Ph
COO*t*Bu
abundance
7.0
6.0
5.0
4.0
3.0
2.0
1.0
0
7.493
7.491
7.488
7.487
7.373
7.371
7.358
7.344
7.325
7.323
7.265
5.094
5.090
3.425
3.416
3.403
3.395
3.383
3.375
3.059
3.032
3.029
2.890
2.870
2.779
2.771
2.761
1.431
1.337
1.305
1.290
1.263
1.257
1.215
1.212
1.200
1.197
0.002
-0.000
X : parts per Million : Proton

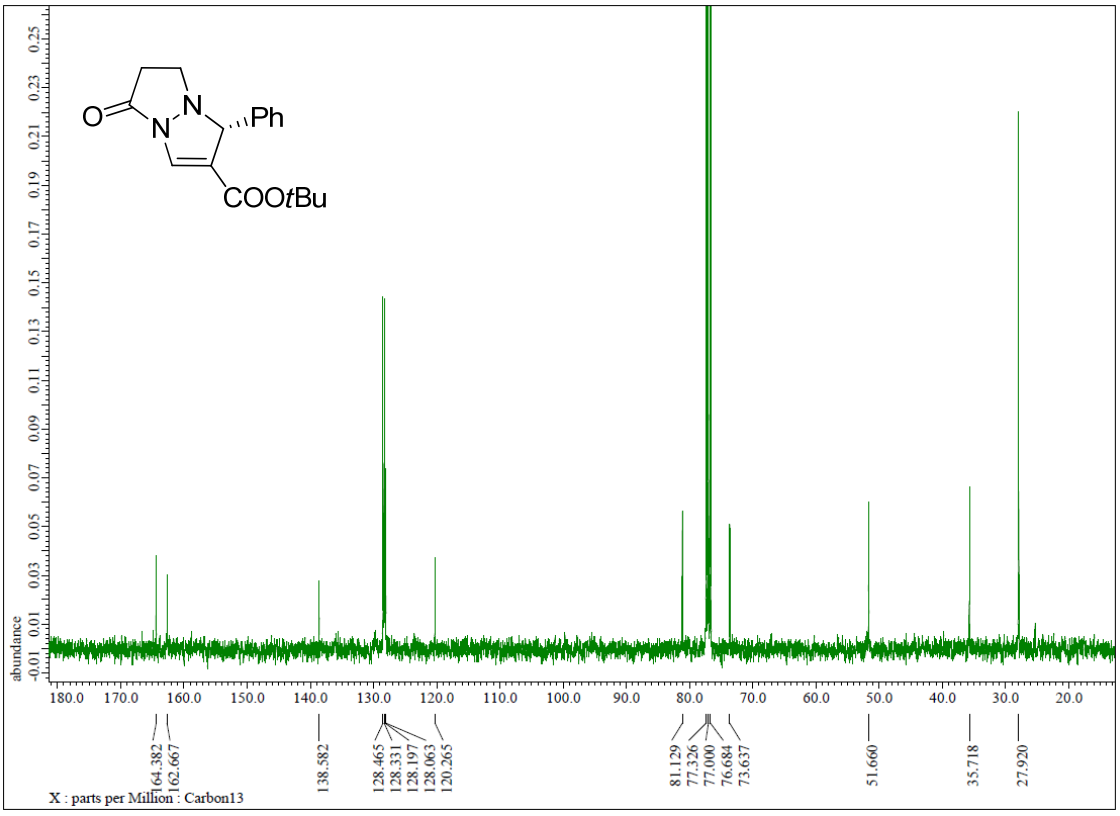
O
N
N
Ph
COO*t*Bu
abundance
180.0
170.0
160.0
150.0
140.0
130.0
120.0
110.0
100.0
90.0
80.0
70.0
60.0
50.0
40.0
30.0
20.0
164.382
162.667
138.582
128.465
128.331
128.197
128.063
120.265
81.129
77.326
77.000
76.684
73.637
51.660
35.718
27.920
X : parts per Million : Carbon13

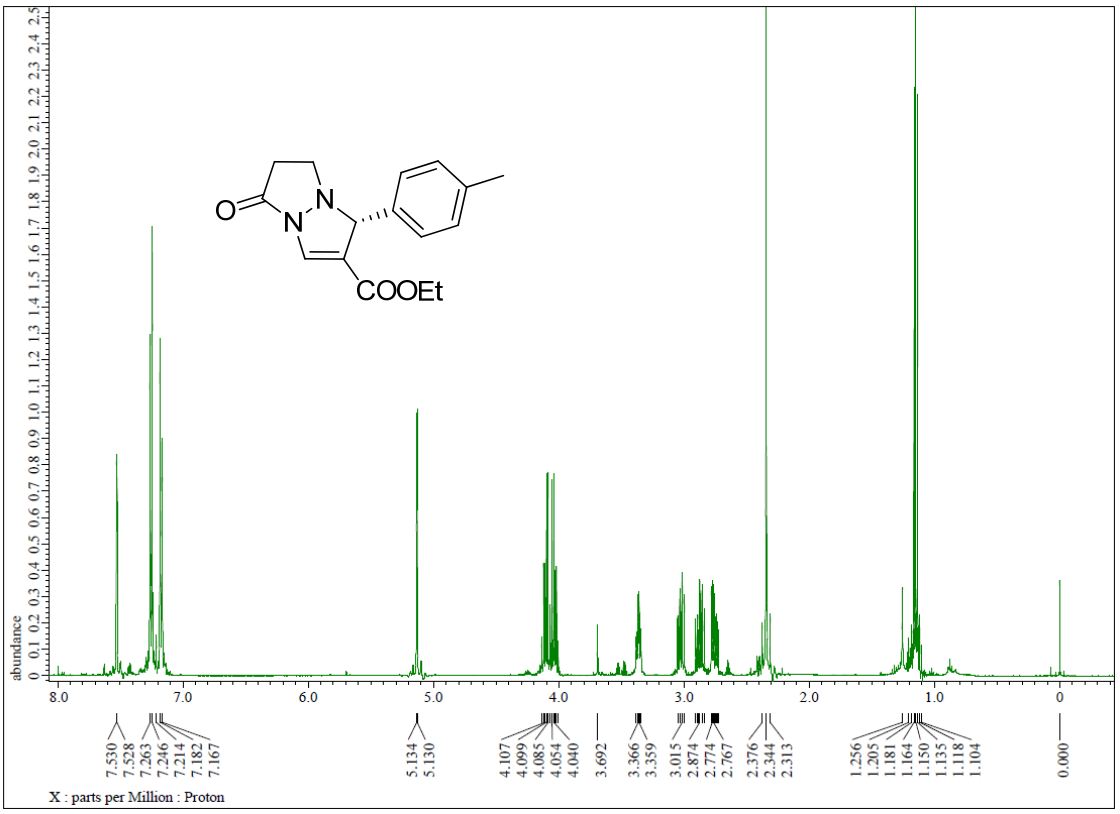
O
N
N
COOEt
abundance
X : parts per Million : Proton
7.530
7.528
7.263
7.246
7.214
7.182
7.167
5.134
5.130
4.107
4.099
4.085
4.054
4.040
3.692
3.366
3.359
3.015
2.874
2.774
2.767
2.376
2.344
2.313
1.256
1.205
1.181
1.164
1.150
1.135
1.118
1.104
0.000

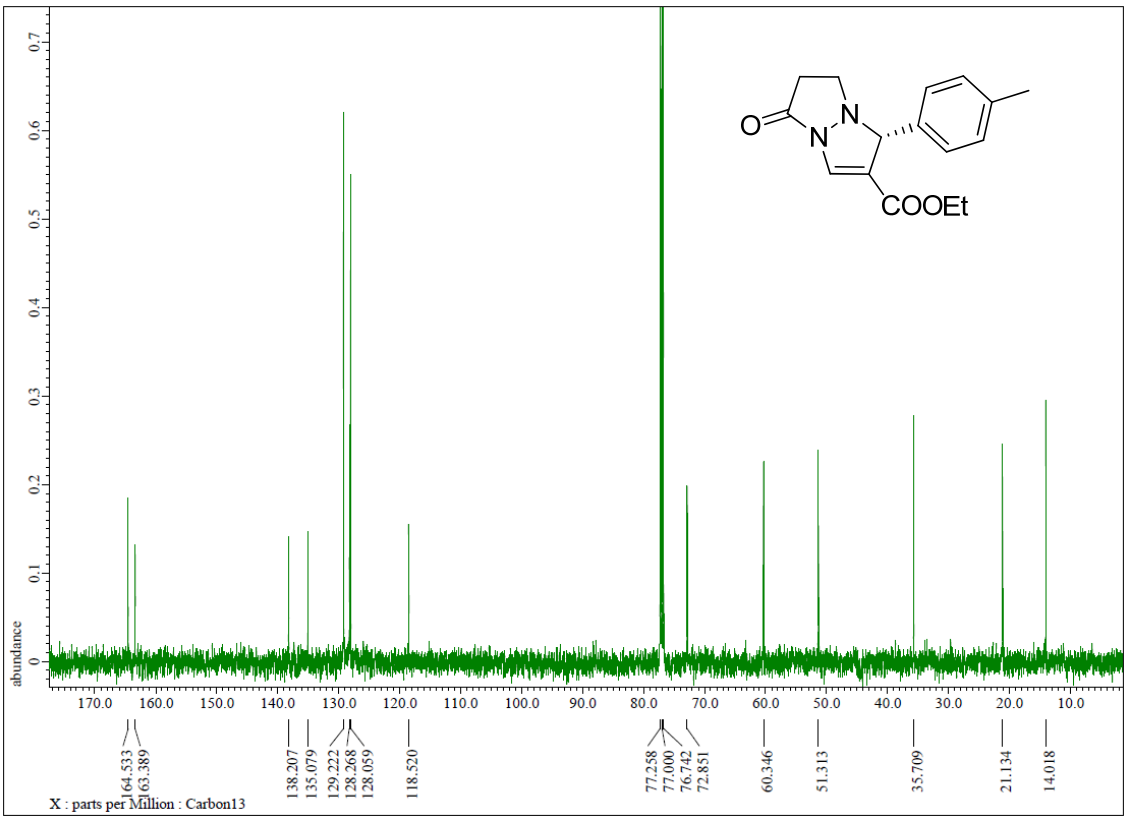
O
N
N
COOEt
abundance
X : parts per Million : Carbon13
164.533
163.389
138.207
135.079
129.222
128.268
128.059
118.520
77.258
77.000
76.742
72.851
60.346
51.313
35.709
21.134
14.018

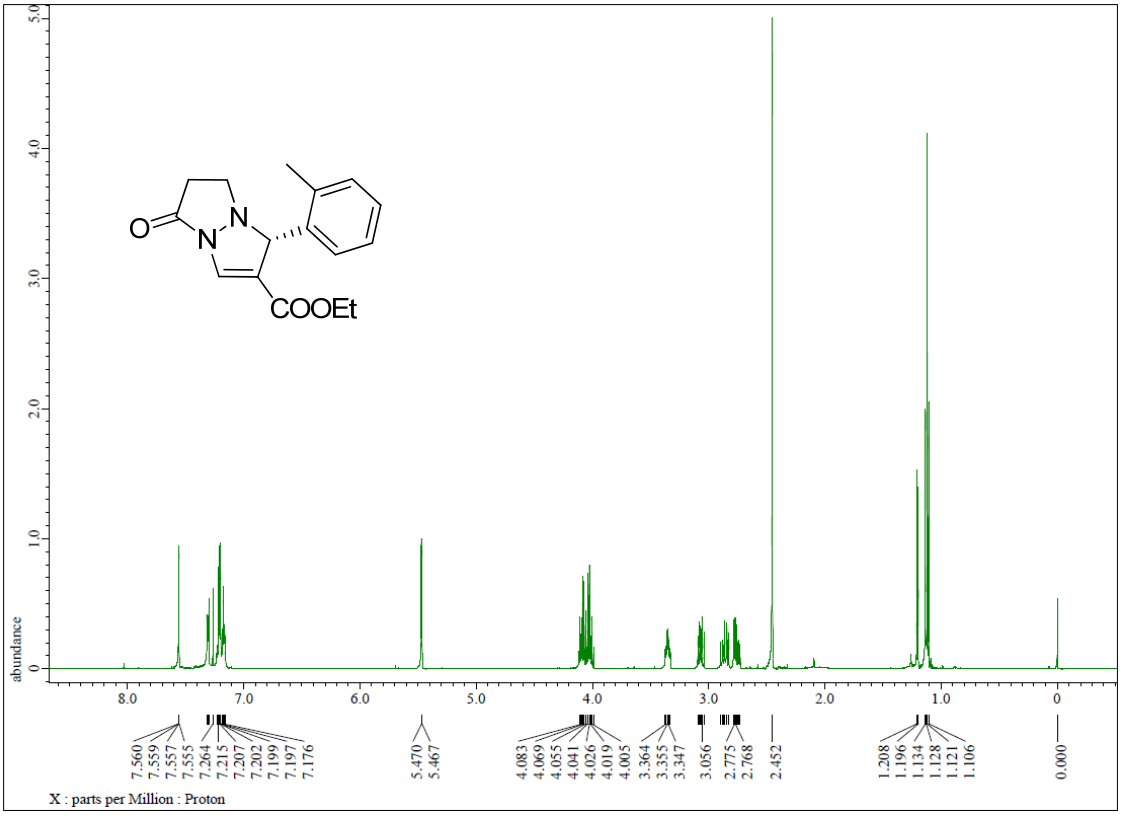
COOEt
abundance
X : parts per Million : Proton
7.560
7.559
7.557
7.555
7.264
7.215
7.207
7.202
7.199
7.197
7.176
5.470
5.467
4.083
4.069
4.055
4.041
4.026
4.019
4.005
3.364
3.355
3.347
3.056
2.775
2.768
2.452
1.208
1.196
1.134
1.128
1.121
1.106
0.000

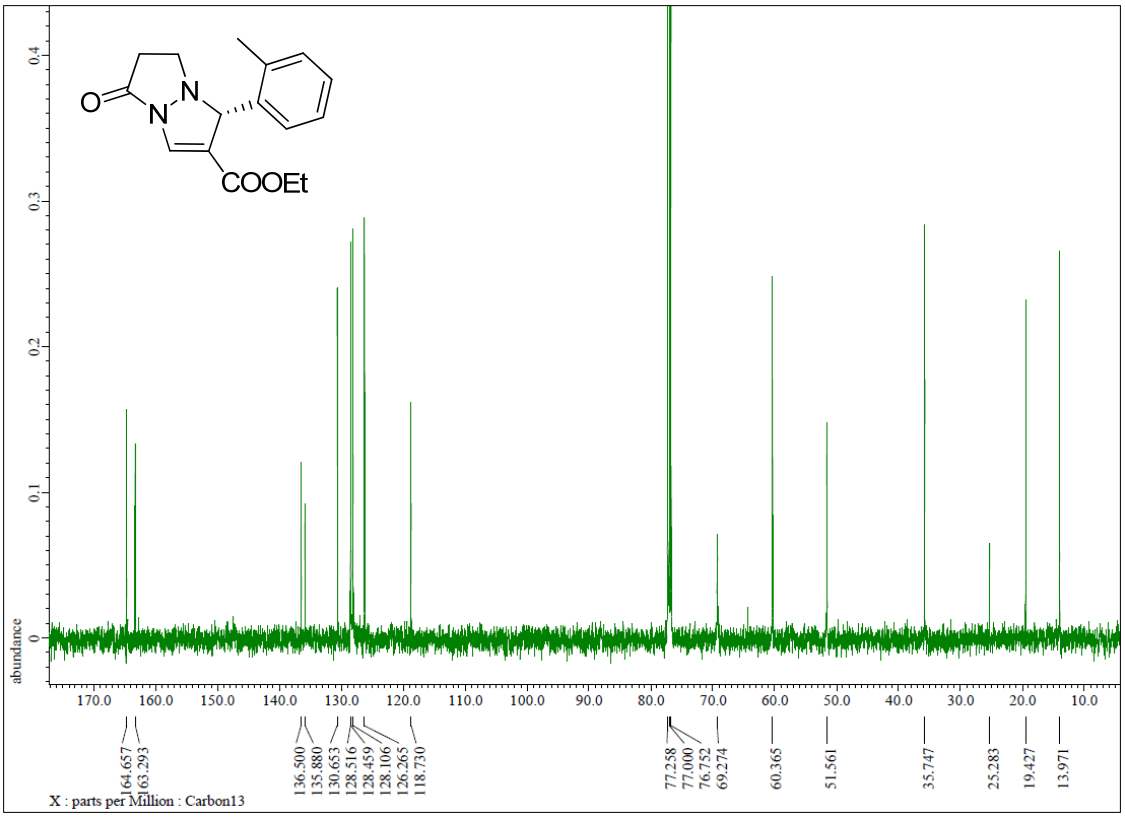
COOEt
abundance
X : parts per Million : Carbon13
164.657
163.293
136.500
135.880
130.653
128.516
128.459
128.106
126.265
118.730
77.258
77.000
76.752
69.274
60.365
51.561
35.747
25.283
19.427
13.971

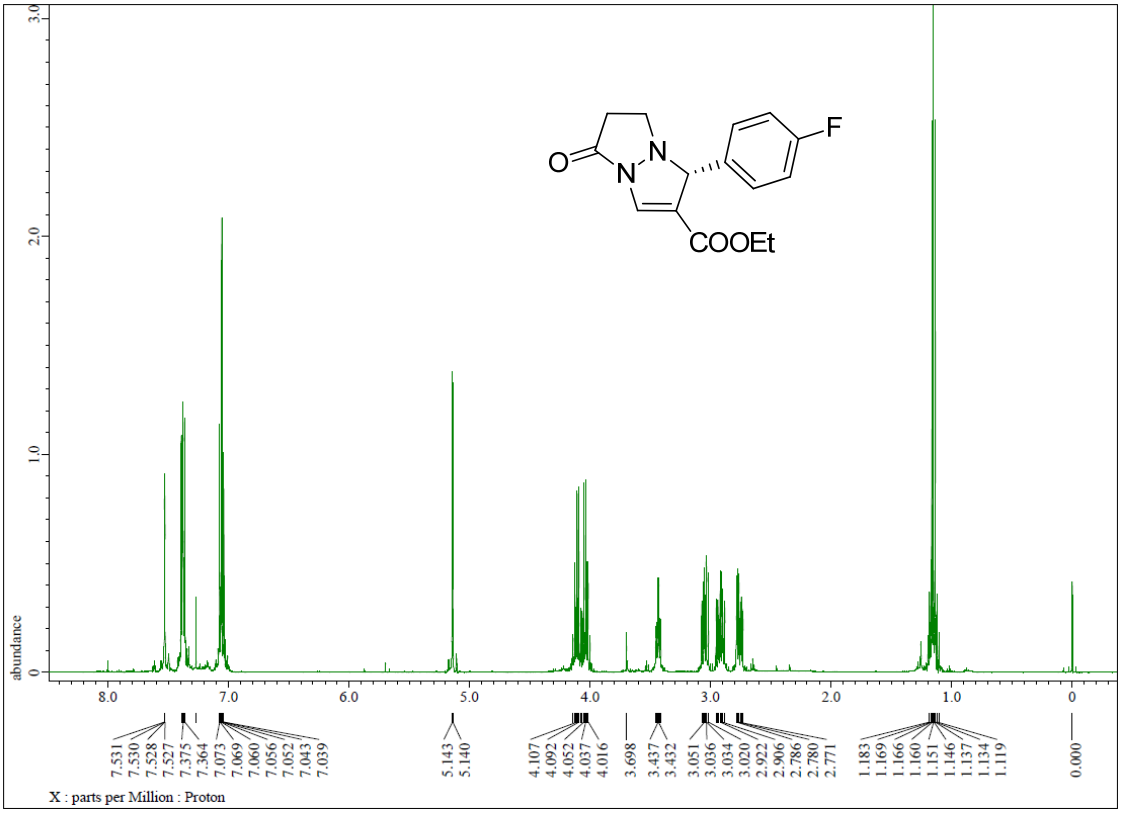
F
O
N
N
COOEt
abundance
X : parts per Million : Proton

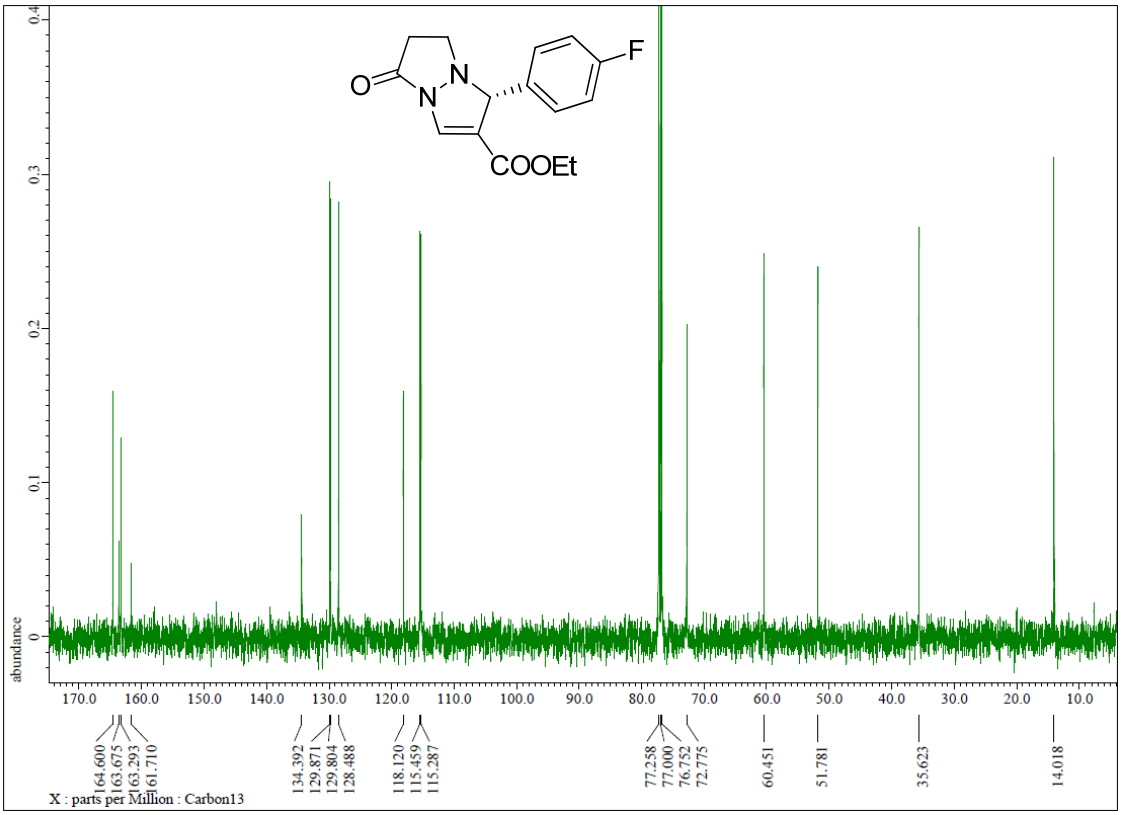
F
O
N
N
COOEt
abundance
X : parts per Million : Carbon13

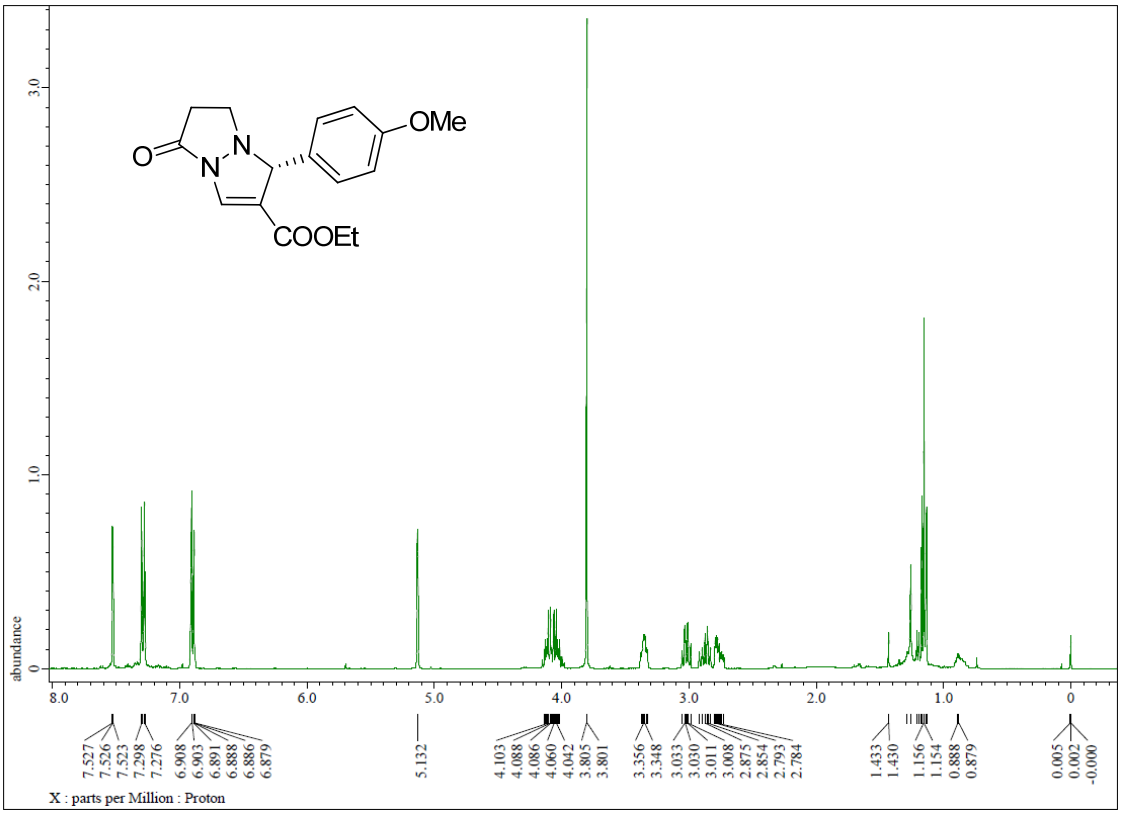
OMe
O
N
N
COOEt
abundance
X : parts per Million : Proton
7.527
7.526
7.523
7.298
7.276
6.908
6.903
6.891
6.888
6.886
6.879
5.132
4.103
4.088
4.086
4.060
4.042
3.805
3.801
3.356
3.348
3.033
3.030
3.011
3.008
2.875
2.854
2.793
2.784
1.433
1.430
1.156
1.154
0.888
0.879
0.005
0.002
-0.000

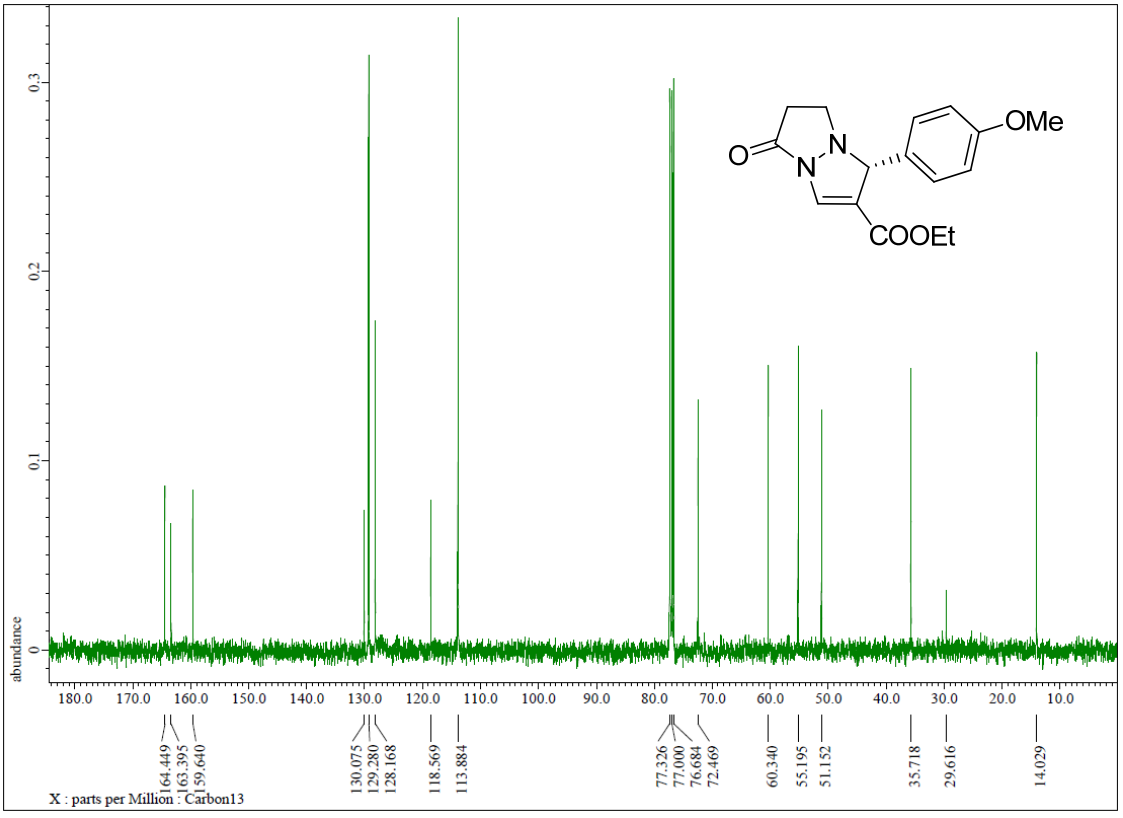
OMe
O
N
N
COOEt
abundance
X : parts per Million : Carbon13
164.449
163.395
159.640
130.075
129.280
128.168
118.569
113.884
77.326
77.000
76.684
72.469
60.340
55.195
51.152
35.718
29.616
14.029

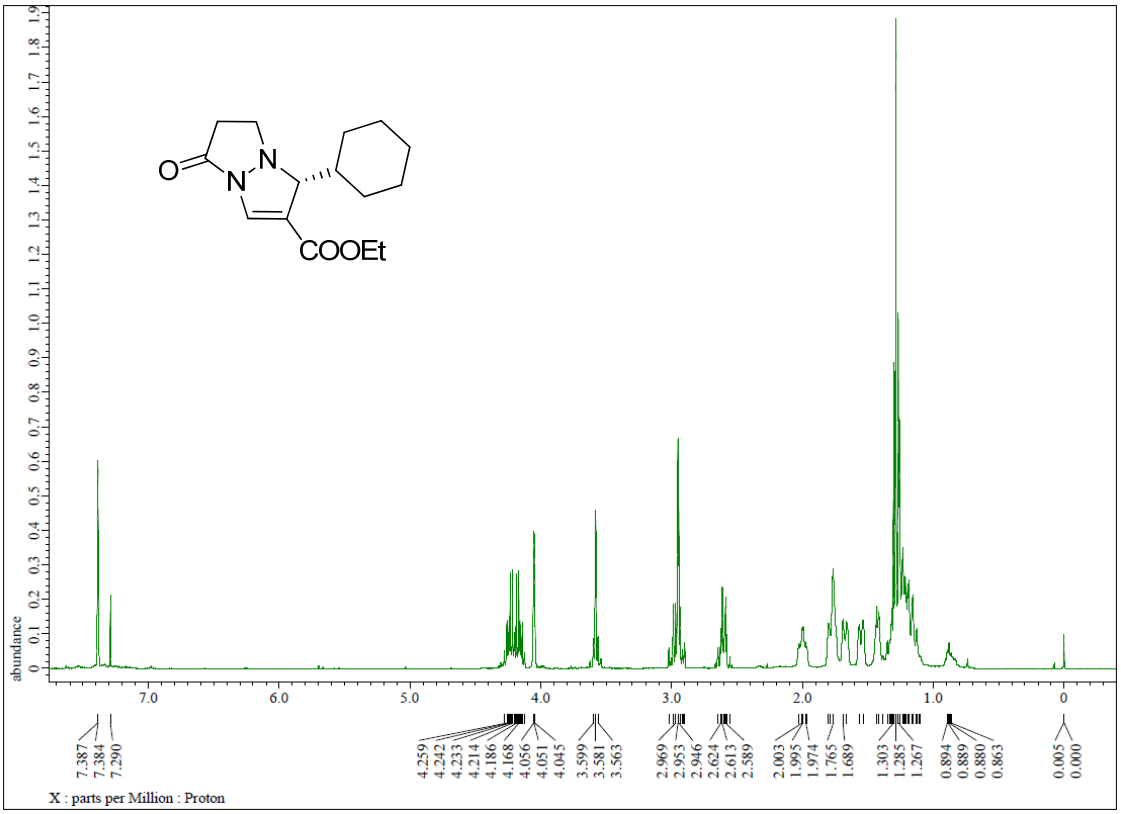
O
N
N
COOEt
abundance
7.387
7.384
7.290
4.259
4.242
4.233
4.214
4.186
4.168
4.056
4.051
4.045
3.599
3.581
3.563
2.969
2.953
2.946
2.624
2.613
2.589
2.003
1.995
1.974
1.765
1.689
1.303
1.285
1.267
0.894
0.889
0.880
0.863
0.005
0.000
X : parts per Million : Proton

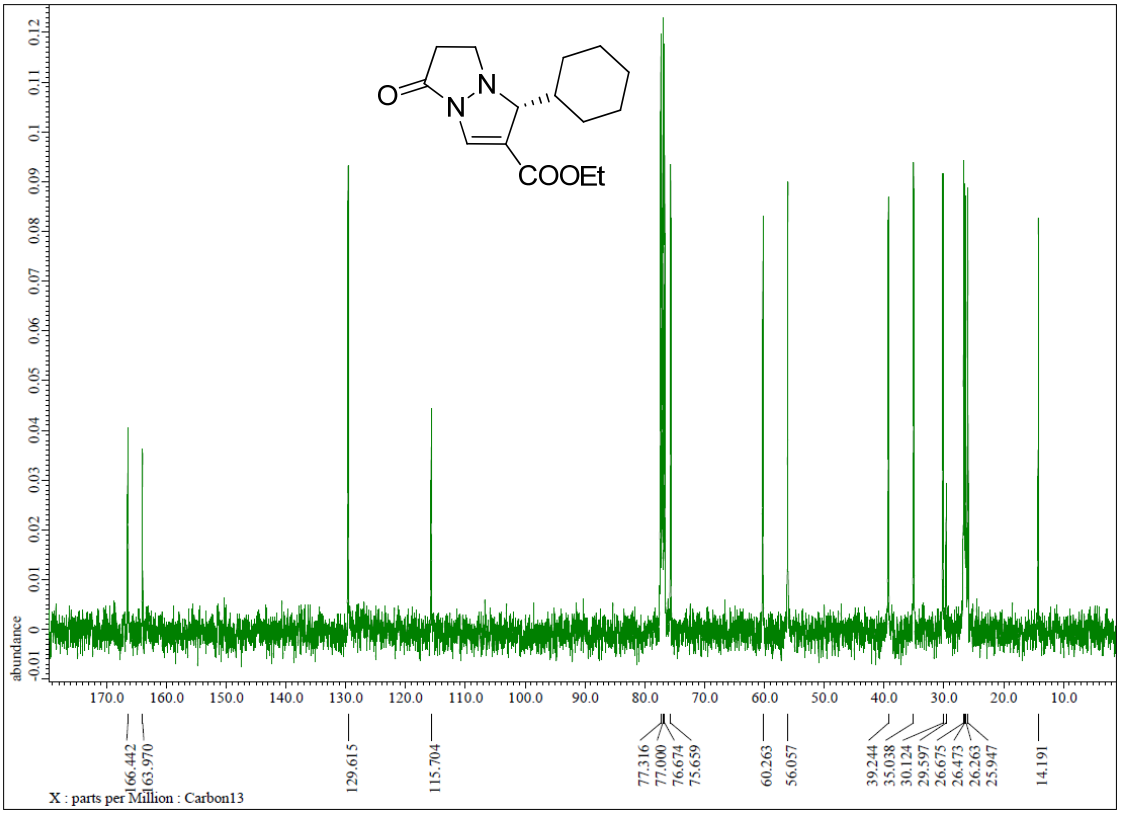
O
N
N
COOEt
abundance
166.442
163.970
129.615
115.704
77.316
77.000
76.674
75.659
60.263
56.057
39.244
35.038
30.124
29.597
26.675
26.473
26.263
25.947
14.191
X : parts per Million : Carbon13

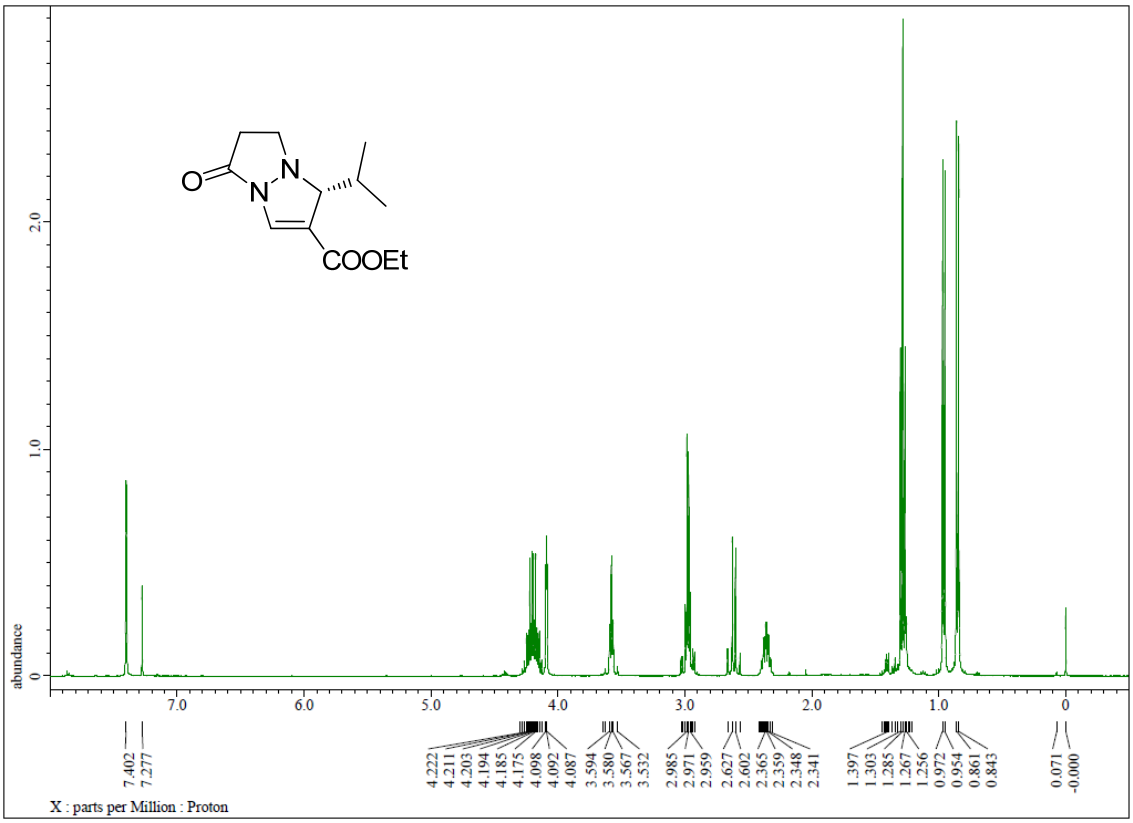
O
N
N
COOEt
abundance
2.0
1.0
0
7.0
6.0
5.0
4.0
3.0
2.0
1.0
0
7.402
7.277
4.222
4.211
4.203
4.194
4.185
4.175
4.098
4.092
4.087
3.594
3.580
3.567
3.532
2.985
2.971
2.959
2.627
2.602
2.365
2.359
2.348
2.341
1.397
1.303
1.285
1.267
1.256
0.972
0.954
0.861
0.843
0.071
-0.000
X : parts per Million : Proton

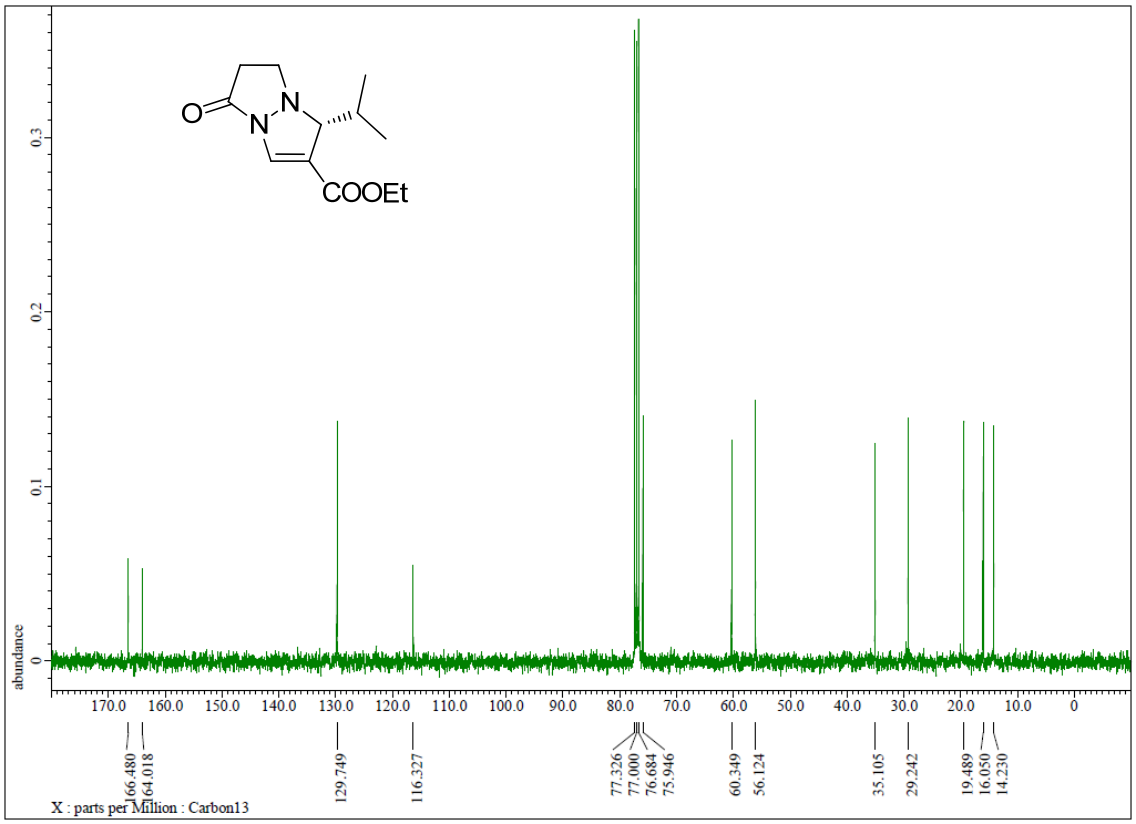
O
N
N
COOEt
abundance
0.3
0.2
0.1
0
170.0
160.0
150.0
140.0
130.0
120.0
110.0
100.0
90.0
80.0
70.0
60.0
50.0
40.0
30.0
20.0
10.0
0
166.480
164.018
129.749
116.327
77.326
77.000
76.684
75.946
60.349
56.124
35.105
29.242
19.489
16.050
14.230
X : parts per Million : Carbon13

9. HPLC data of [3+2]-cycloadducts

(Table 2, entry 1)

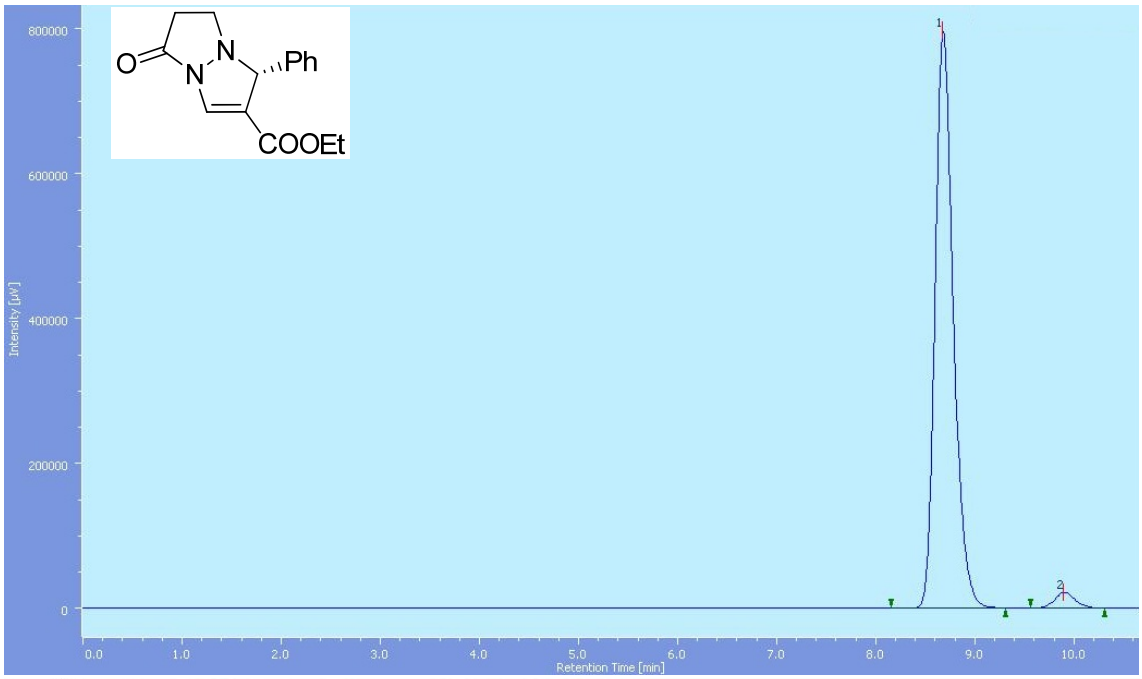

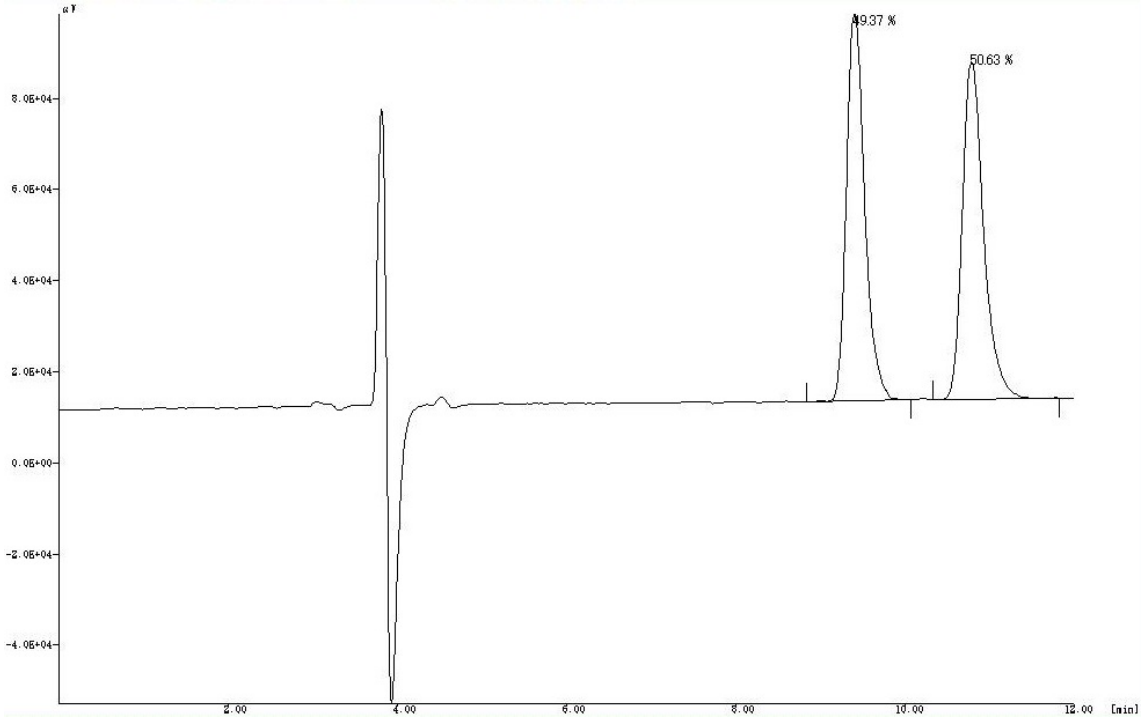

(Table 2, entry 2)

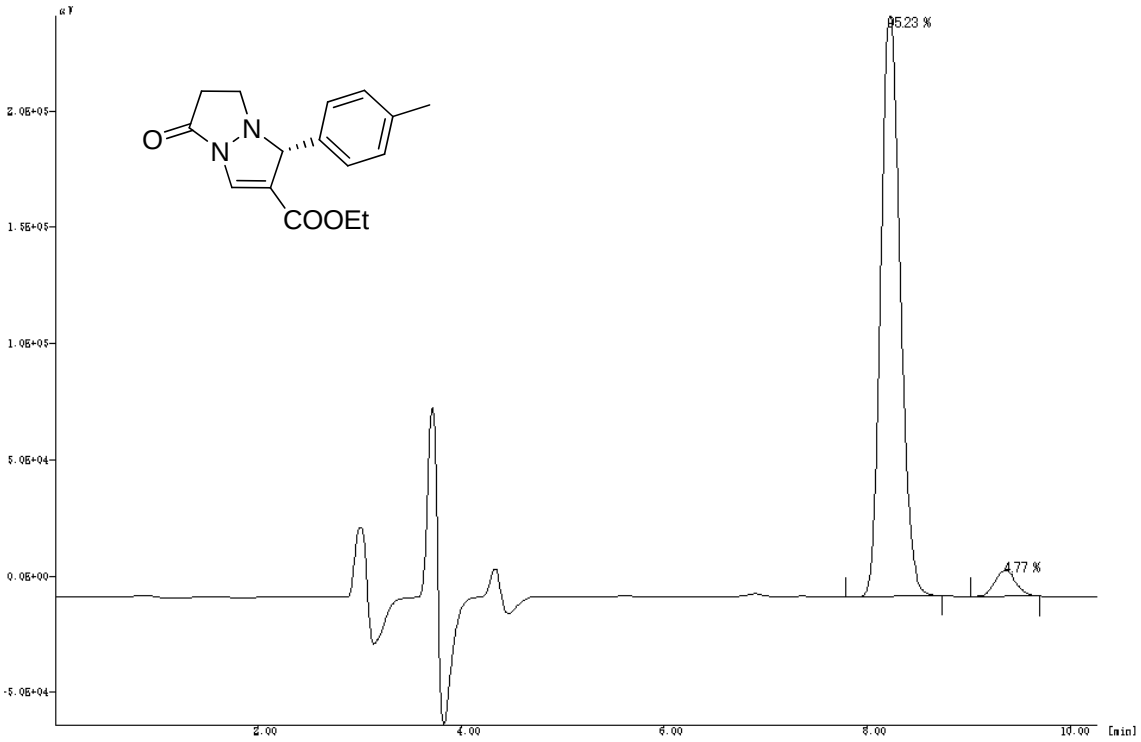

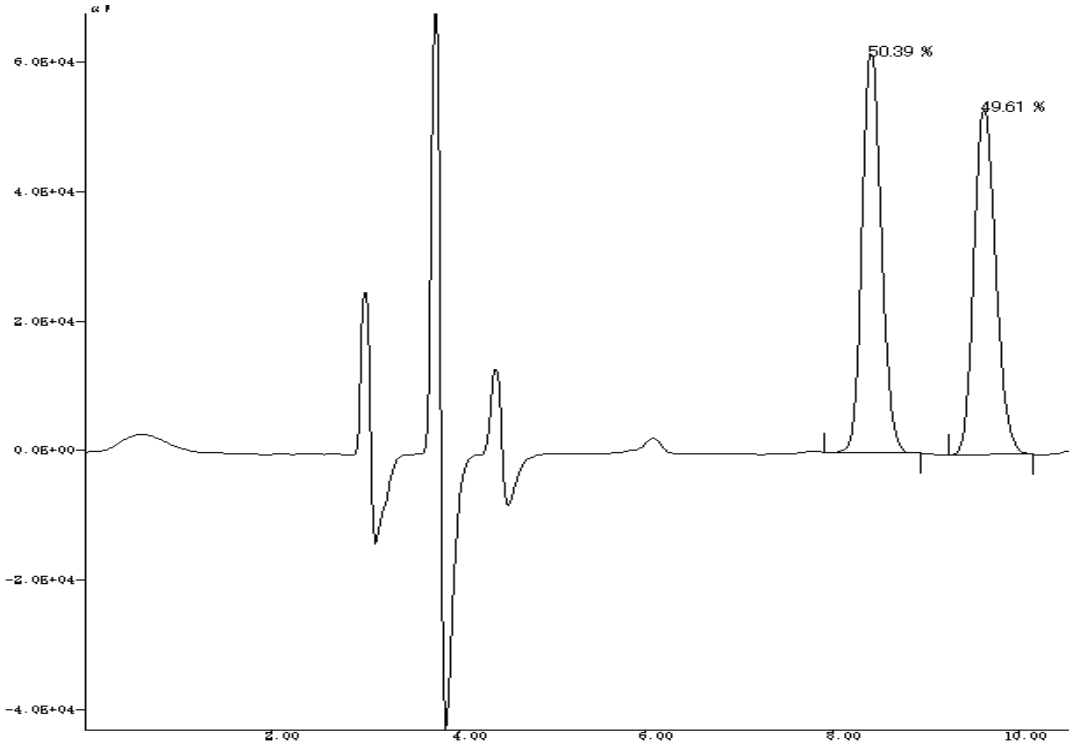

(Table 2, entry 3)

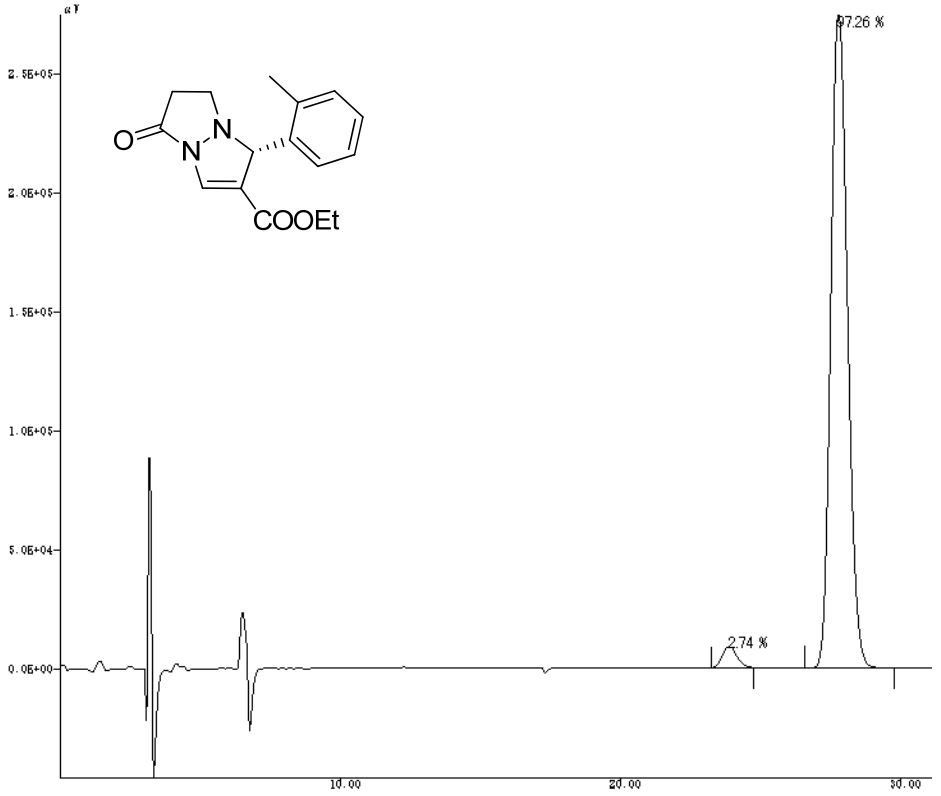

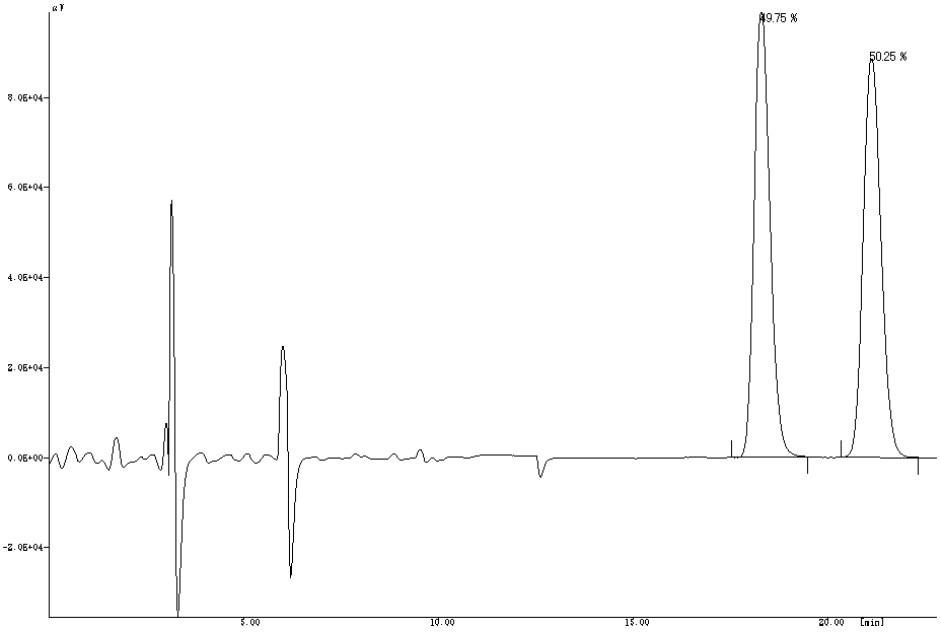

(Table 2, entry 4)

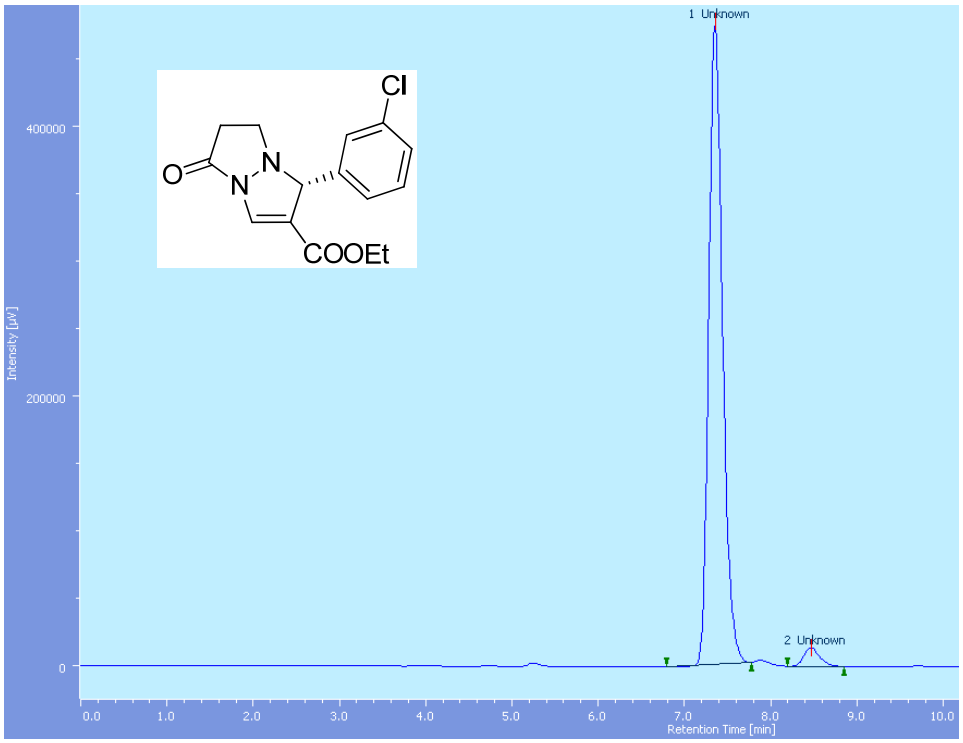

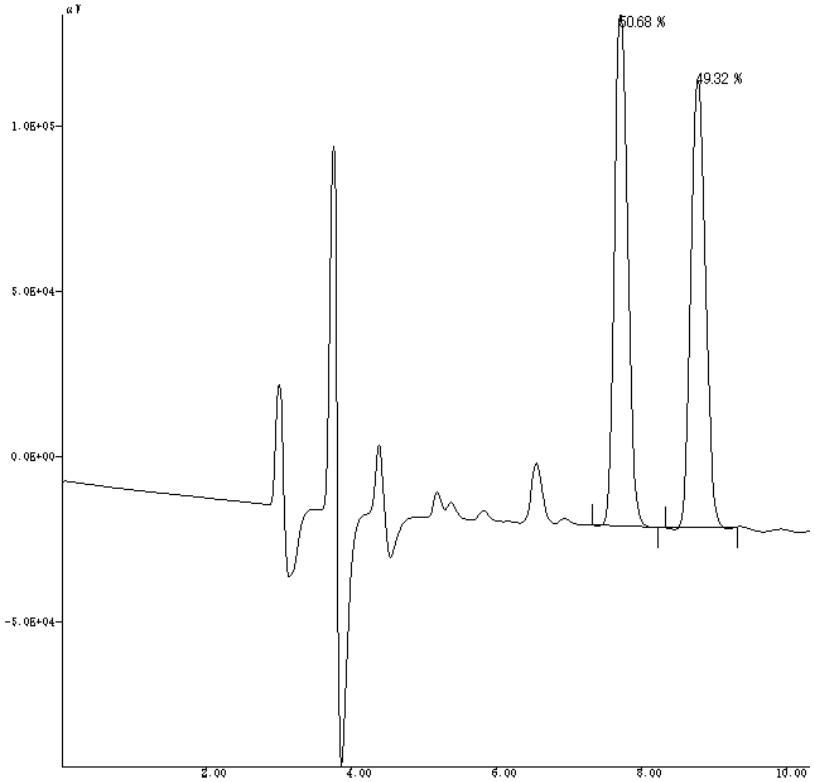

(Table 2, entry 5)

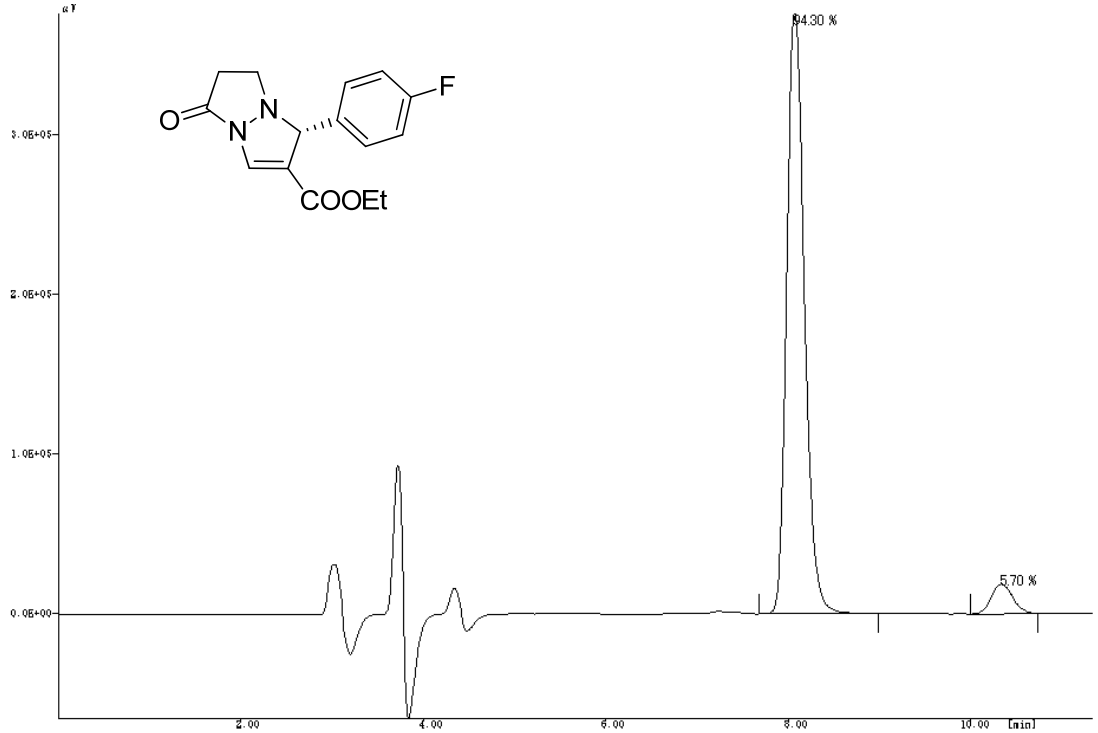

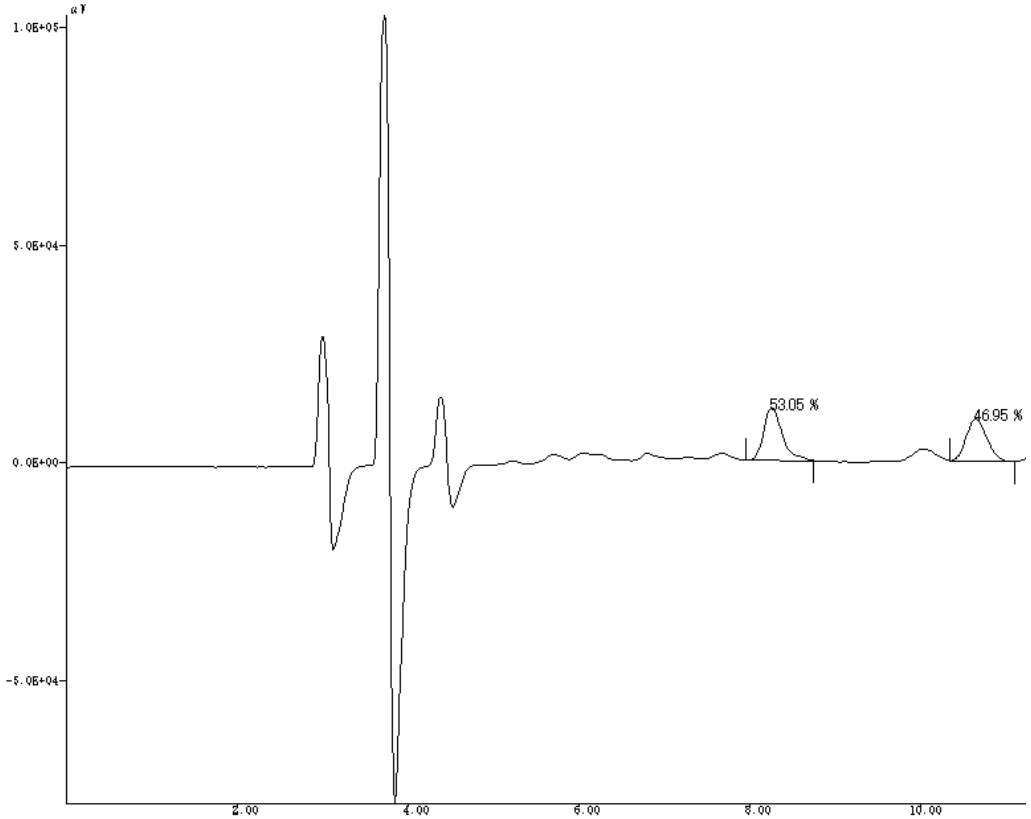

(Table 2, entry 6)

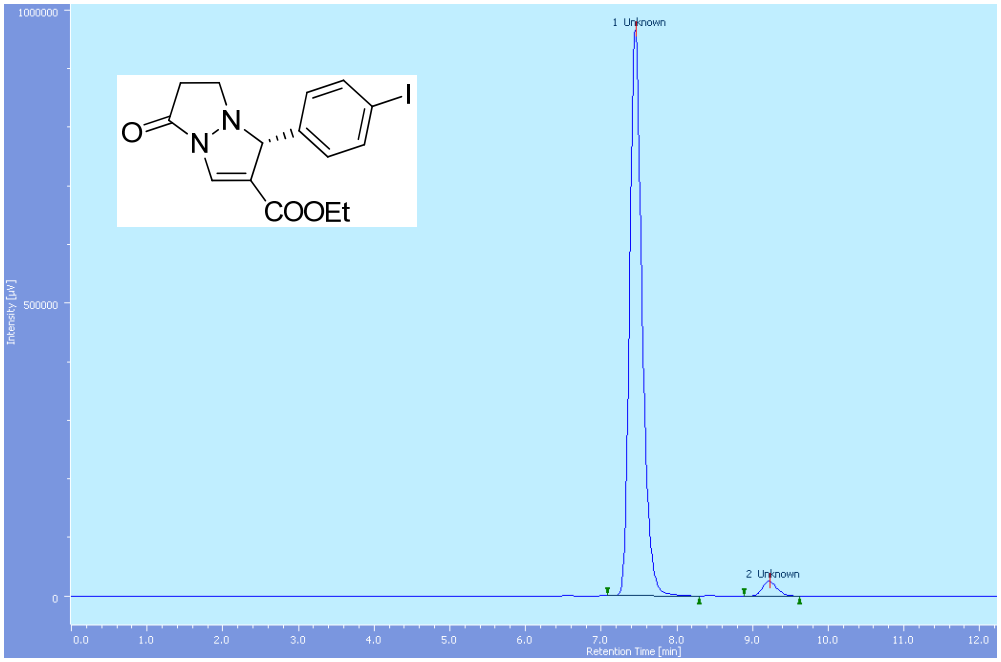

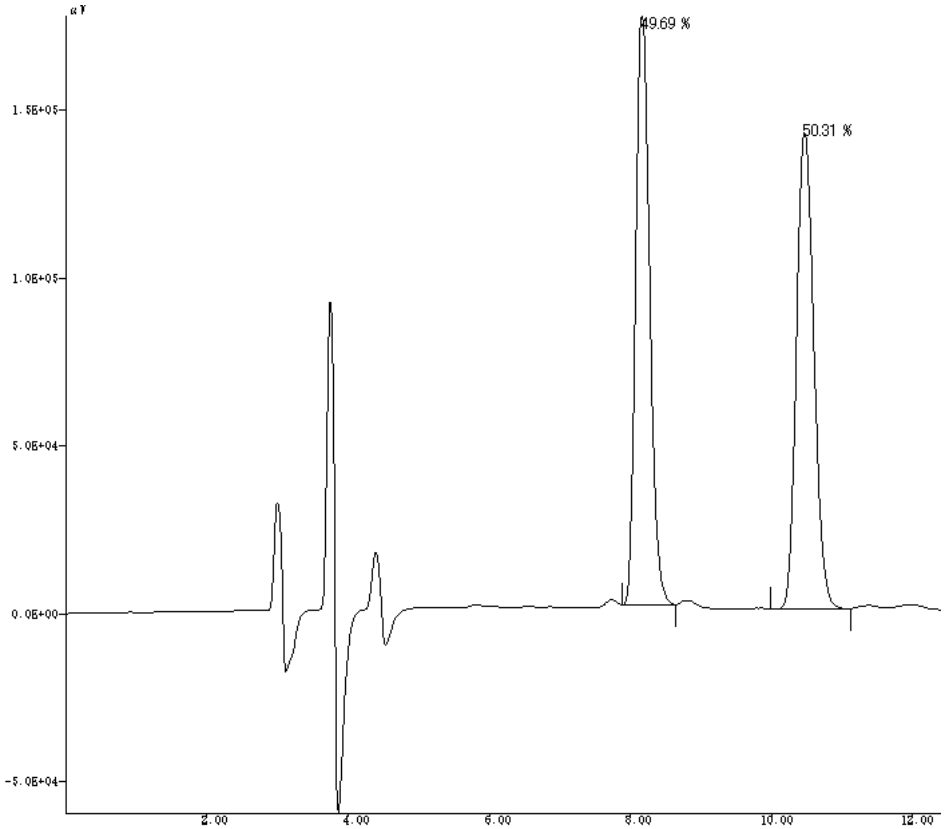

(Table 2, entry 7)

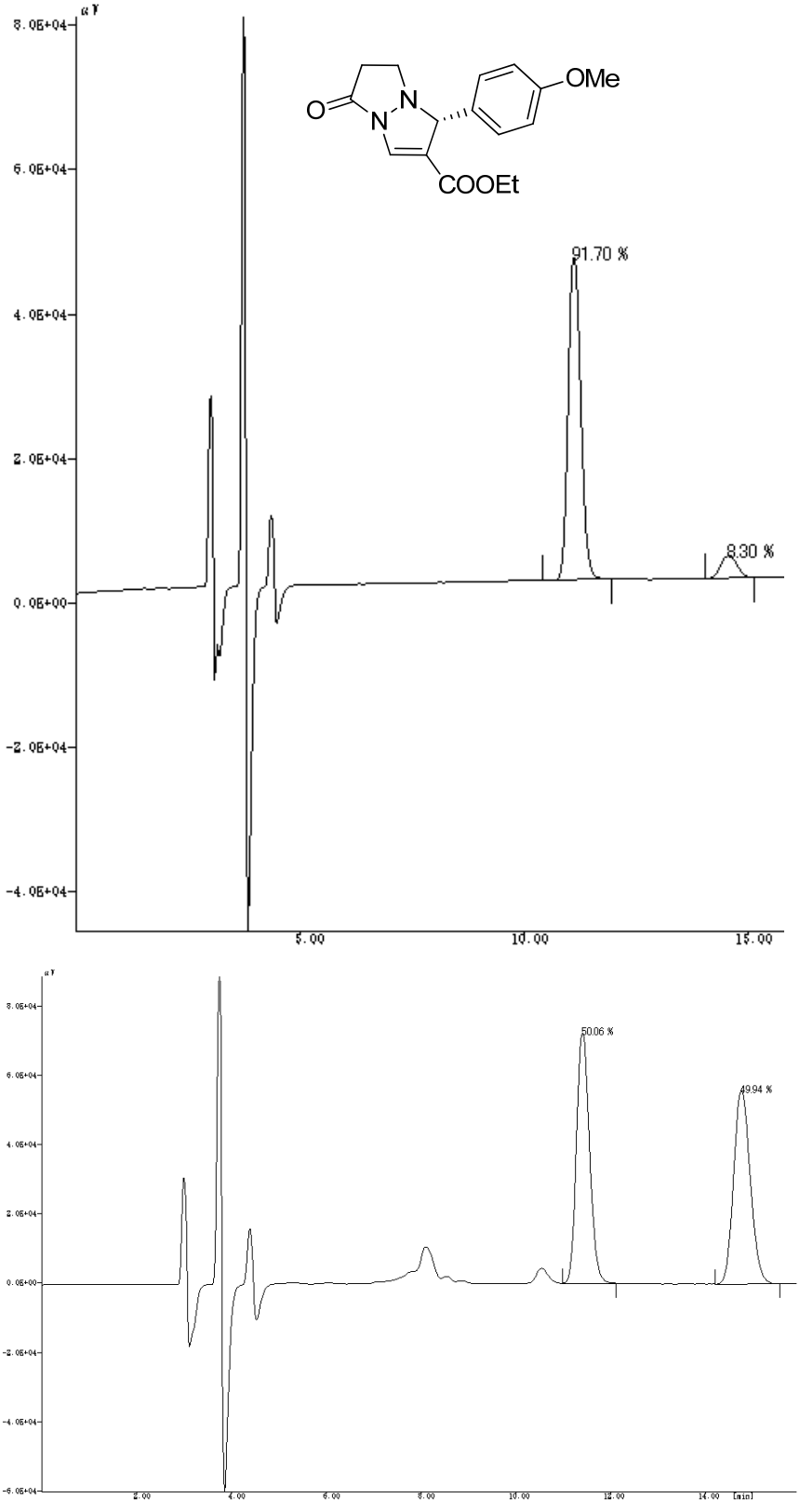

(Table 2, entry 8)

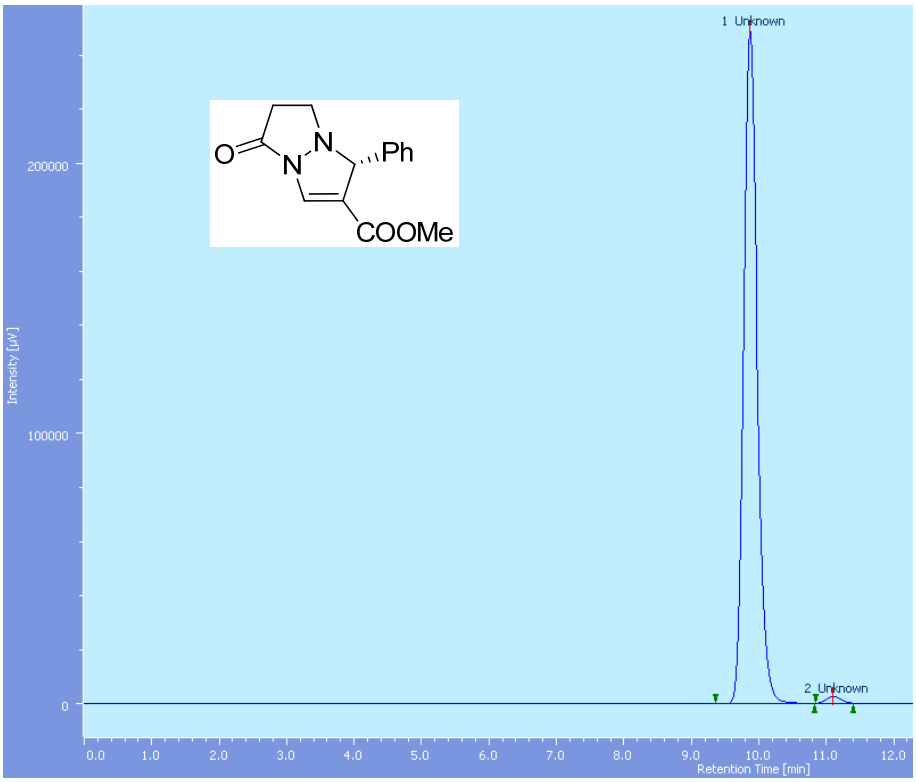

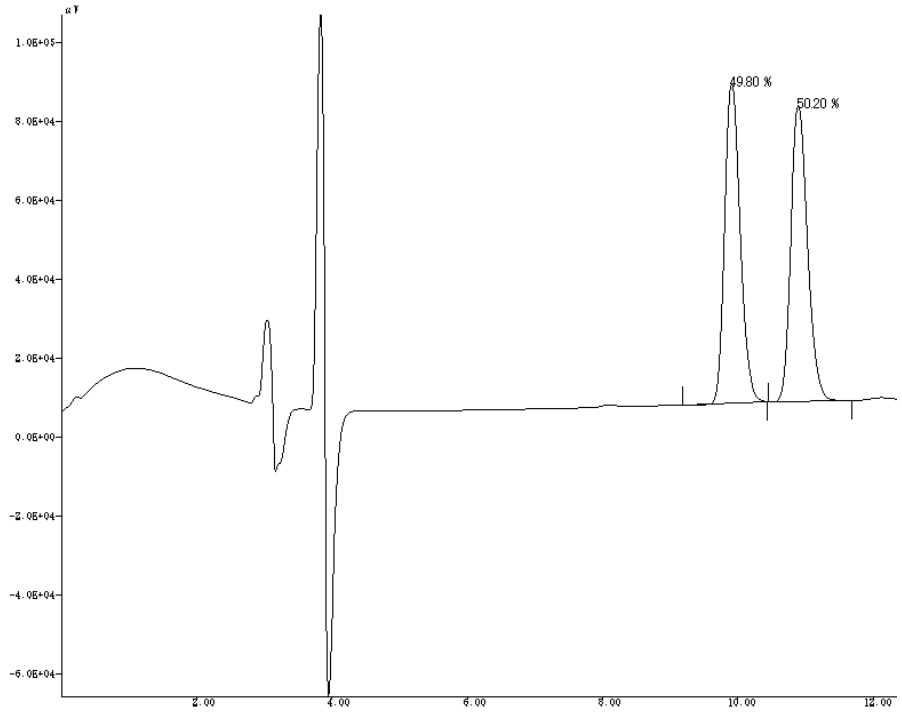

(Table 2, entry 9)

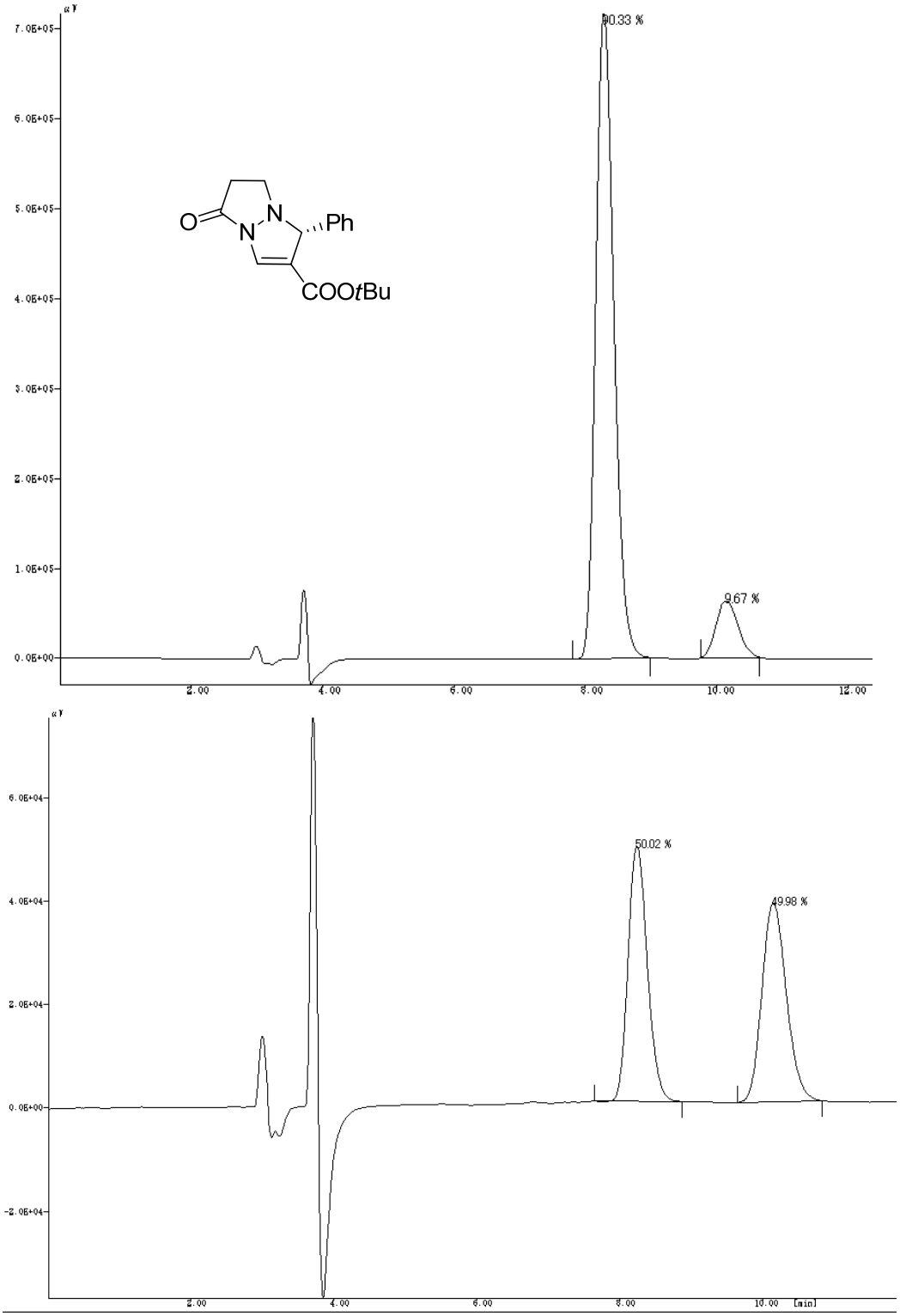

(Table 2, entry 10)

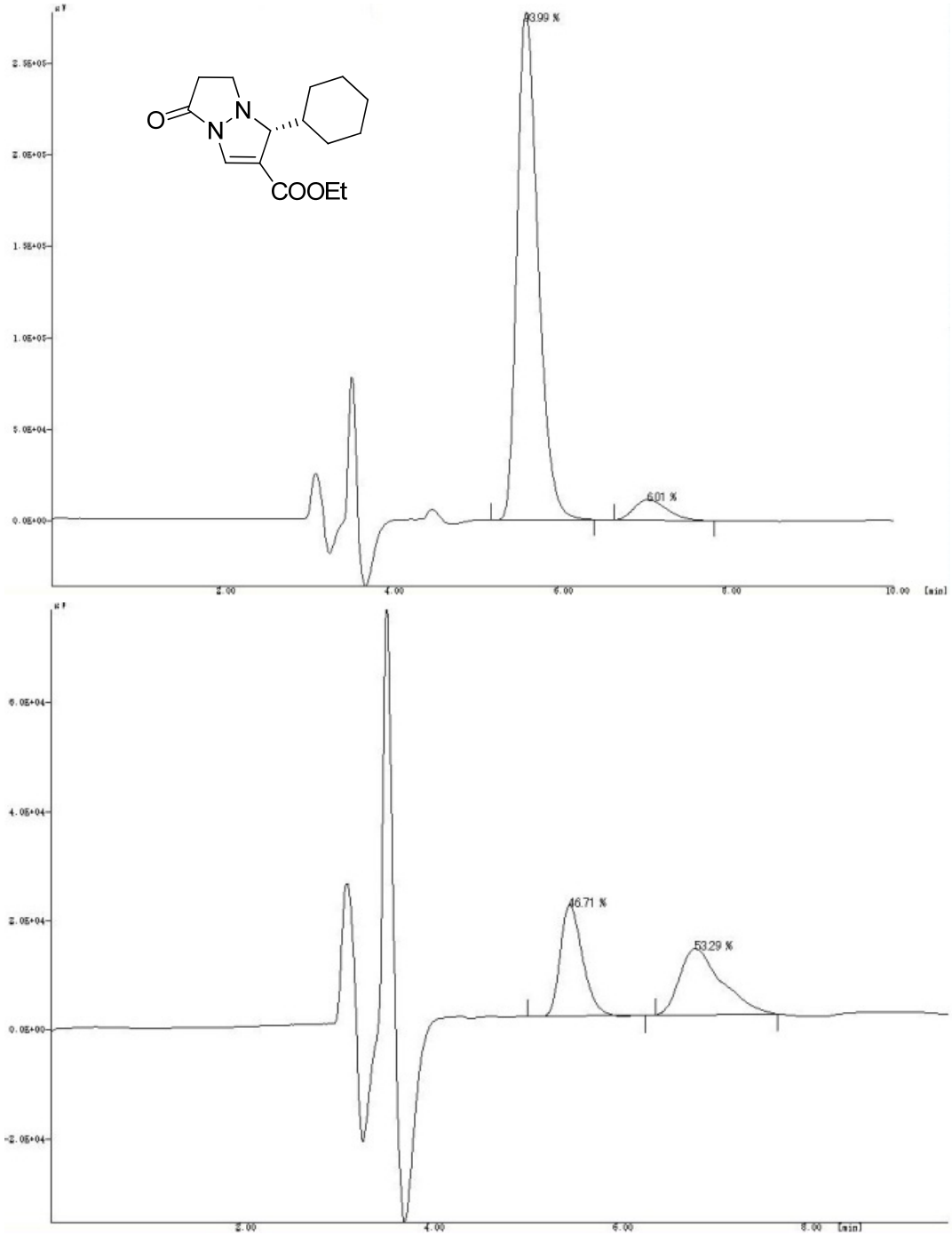

(Table 2, entry 11)

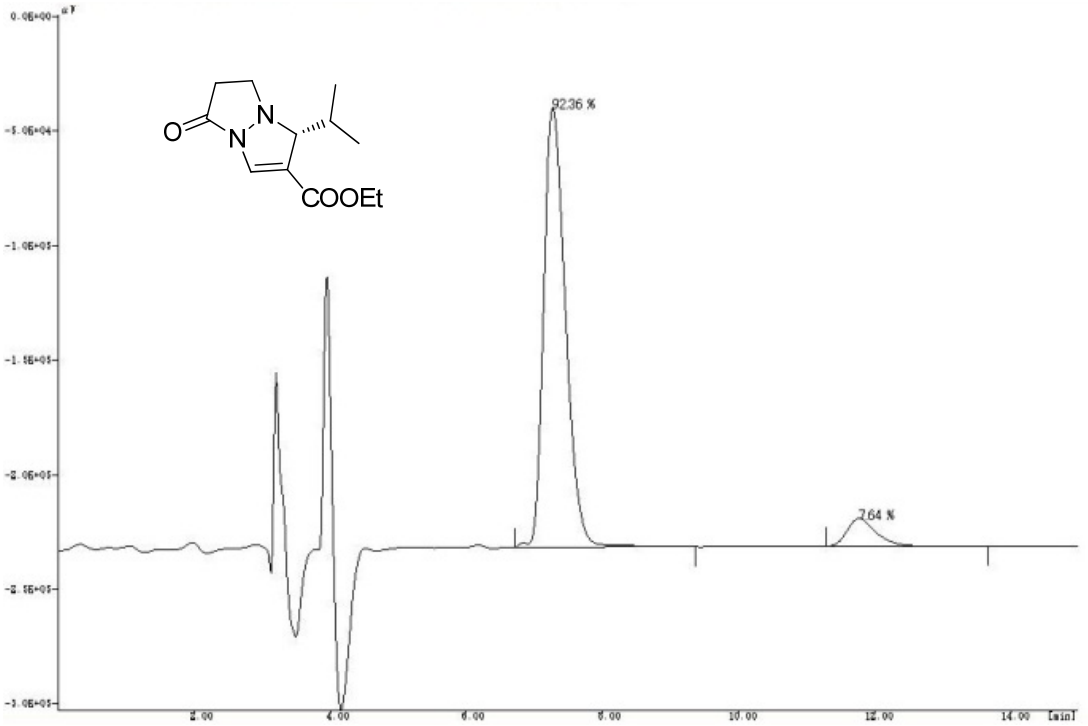

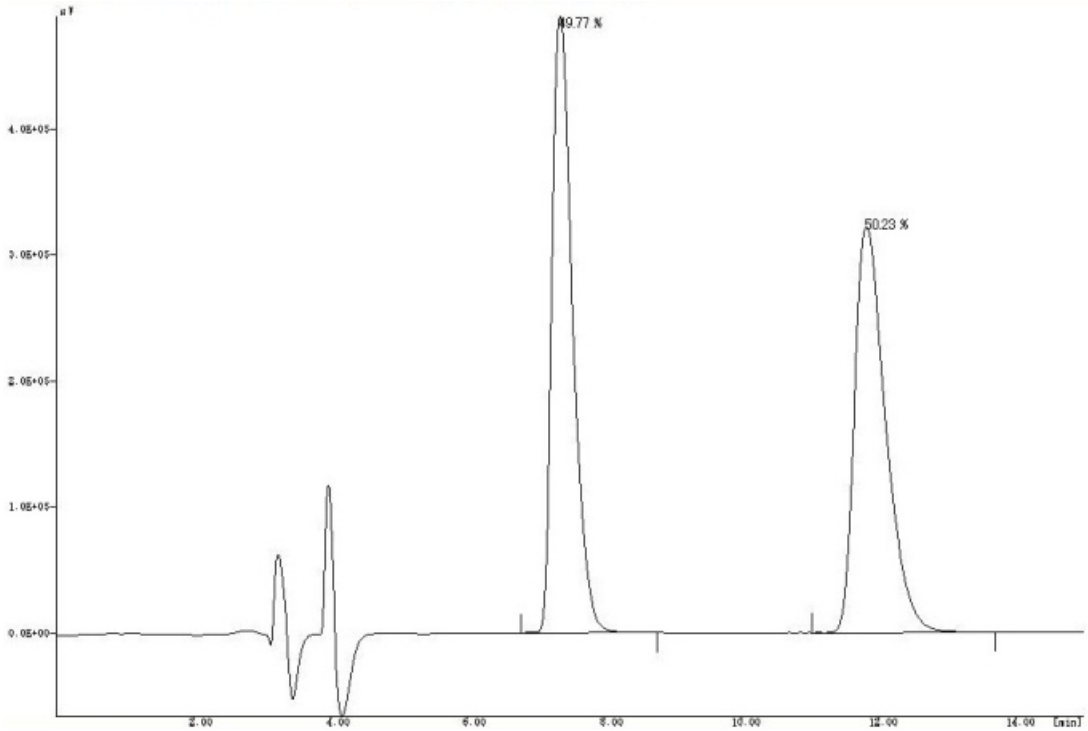

10. Proposed model of PyBodine(Ala)-Cu(OAc)$_2$ catalyzed [3+2]-cycloaddition